1   **Sea dynamics impacts on the macroaggregates:**

2   **a case study of the 1997 mucilage event in the northern Adriatic**

3   Romina Kraus and Nastjenjka Supić

4

5   **ABSTRACT**

6

7   The massive formations of mucilaginous macroaggregates of various forms and

8   dimensions are typical for the northern Adriatic (i.e., mucilage phenomenon). In this work we

9   analysed the 1997 mucilage event and showed that macroaggregates were formed in the upper

10   layers of the water column in the central parts of large gyres and were dispersed from their

11   origin by geostrophic currents. Beside *Cylindrotheca closterium*, an already established regular

12   opportunistic species of the mucilage phenomenon, originating from the sediment, we detected

13   another benthic species, *Thalassionema nitzschioides*, of a sporadic character. Both were

14   present in scarce amounts in the water column at the time of sampling first macroaggregates,

15   but reached high abundances after/close to the mucilage event ending. Several surface heat loss

16   were documented during the period of investigation. The first one, and the most intense,

17   occurred on 18 July (heat loss over 250 W m, during episode of NW wind), in time of the first

18   macroaggregates formation (first macroaggregates sampled on 22–23 July), induced intense

19   turbulent mixing near the bottom and introduced *C. closterium* from sediment into the water

20   column. *T. nitzschioides* was already present in the water column in central part of the region

21   on 8 July and was included in the first macroaggregates, which were dispersed westwards and

22   eastwards after the 18 July heat loss episode which changed circulation pattern. The later, less

23   intense, surface heat loss episodes, induced mostly by NE winds, were efficient in tearing

24   already formed macroaggregates, inhabited with opportunistic species, and induced their

25   release from a macroaggregate into the surrounding water column. The mucilage event

26   drastically changed the phytoplankton composition in the water column with increased

27   abundance of the opportunistic species at the time of macroaggregates decay. In addition, winds

28   from NE were responsible for drawing lower salinity waters, with its specific species

29   community and in which macroaggregates were already formed, towards eastern coast

30   extending the event to large area. In addition to aforementioned findings, our investigation

31   resulted in two hypothesis. First, summer surface heat loss episodes play a role in sustaining

32   mucilage events by introduction of *C. closterium* from the sediment and/or decaying

33 macroaggregates in the water column. Second, geostrophic currents are important in spreading

34 of various types of aggregates, including marine snow, with consequent spreading of species

35 over the wider marine areas.

36

37 **Keywords**

38 mucilage event, macroaggregates, geostrophic currents, northern Adriatic, *Cylindrotheca*

39 *closterium, Thalassionema nitzschioides*

40

41 **1. INTRODUCTION**

42 The mucilage phenomenon is an event typical of the northern Adriatic (further in text:

43 NA), characterised by the massive formation of white to brownish, amorphous, sticky,

44 mucilaginous macroaggregates (further in text: macroaggregates) of various forms and

45 dimensions, ranging from 0.5 cm to several km in diameter. Small types of macroaggregates,

46 flocs (0.5-1 cm) and macroflocs (1-5 cm) are ubiquitous and present in the water column year-

47 round with extremely variable abundances and are commonly known as marine snow

48 (Alldredge and Silver, 1988; Stachowitsch et al., 1990; Precali et al., 2005). Large type

49 macroaggregates are present only during mucilage events in various abundances and include

50 elongated types: stringers (few mm x 2 – 25 cm) and ribbons (few cm x 10/20 cm – 1 m),

51 amorphous forms: clouds (diameter 0.5 – 3/4 m) and layers of various dimensions: cowebs,

52 false bottoms, blankets, creamy or gelatinous surface layers. Large macroaggregates spread

53 over wide areas of the sea surface or throughout the water column, even for as much as hundreds

54 of kilometres (Stachowitsch et al., 1990, Degobbis et al., 1999; Precali et al., 2005).

55 Although occasional occurrences of the mucilage events were observed in Dalmatian,

56 Greek, Tyrrhenian and Sicilian coastal areas (Stachowitsch et al., 1990; Calvo et al., 1995;

57 Gotsis-Skretas, 1995; Innamorati, 1995), they were neither as frequent, nor of such an enormous

58 scale, as are those occurring in the NA. According to the gathered observations from an

59 assortment of popular and scientific publications, the first record of mucilage phenomenon in

60 the NA dates back to 1729, followed by occurrences in 1872, 1880, 1891, 1903, 1905, 1920-

61 1922, 1924, 1927, 1929, 1930, 1935, 1941, 1949, 1951, 1959, 1973, 1976 and 1983 (Fonda-

62 Umani et al., 1989; Danovaro et al., 2009). Based on available records, it seems that in the last

63 period mucilage event recurred more often: in 1988 – 1991, 1997 an year by year in periods

64 2000 – 2004 and 2006 – 2008 (Degobbis et al., 1999; Precali et al., 2005; Danovaro et al.,

65 2009).

66   Unusual bloom in the English Channel, massive foam production noticed in the North

67   Sea or a mass accumulation of the mucilage in Tasman Bay of New Zealand have all been easily

68   attributed to specific phytoplankton species such as *Chaetoceros wailesii*, *Phaeocystis* or

69   *Gonyaulax hyaline*, respectively, due to coinciding massive abundances of the mentioned

70   species (Fogg, 1995; Lancelot, 1995; MacKenzie et al., 2002). On the contrary, for the mucilage

71   event occurring in the winter of 2007/08 in the Sea of Marmara, several diatoms and

72   dinoflagellates were related to the event (Aktan, et al., 2008; Tüfekçi et al., 2010). In contrast,

73   no specific species coinciding with the mucilage events occurring in the NA were ever

74   identified (Pistocchi et al., 2005). During macroaggregates formation process, a wide range of

75   organisms coincidently inhabiting the ambient water (Revelante and Gilmartin, 1991; Flander-

76   Putrle and Malej, 2008) get entrapped in the newly formed matrix of the suspended organic and

77   inorganic material, generated by gelling of mainly microphytoplankton exuded

78   polysaccharides, primarily diatoms (Degobbis, 1989; Stachowitsch et al., 1990; Kaltenbock and

79   Herndl, 1992; Kovac et al., 2002). Although the macroaggregates microphytoplankton

80   composition varied from one event to another, the main contributors were recurrently diatoms

81   (Herndl and Peduzzi, 1988; Stachowitsch et al., 1990; Rinaldi et al., 1995; Fonda Umani et al.,

82   2005; Totti et al., 2005). Species present in macroaggregates are typical members of the

83   spring/summer phytoplankton community of the NA (Revelante and Gilmartin, 1976;

84   Revelante et al., 1984; Totti et al., 2005). In the newly formed macroaggregates, phytoplankton

85   community and relative abundances of dominant species resemble those in the ambient water

86   (Najdek et al., 2002, 2005; Flander-Putrle and Malej, 2008). After the formation, the

87   macroaggregate embodies a self-sustaining ecosystem with the internal primary production and

88   organic matter recycling (Revelante and Gilmartin, 1991; Degobbis et al., 1995; Najdek, 1996),

89   enabling pronounced inside transformations, alternations and species successions, generally

90   dissimilar to the ones ongoing in the ambient water (Revelante and Gilmartin, 1991; Decho and

91   Herndl, 1995; Najdek et al., 2002). It is hypothesised that macroaggregates have a relatively

92   long residence time of one to three months as their species composition progressively changes

93   with age and from the one characterising the ambient water (Fogg, 1995). With the

94   macroaggregate age, abundance of all organisms comprised within was observed to increase

95   for several orders of magnitudes (from 1 to 3, even up to 5) from their abundance in the seawater

96   at the time of the macroaggregate formation (i.e., origin) and independently from the concurrent

97   surrounding water (e.g., Alldredge and Silver, 1988; Revelante and Gilmartin, 1991; Del Negro

98   et al., 2005; Totti et al., 2005). In addition, macroaggregates were found to differ from the

99   ambient water in relative proportions of dominant species (Revelante and Gilmartin, 1991) or

100   to differ in species composition completely (Cataletto et al., 1996). Based on findings that

101   seawater phytoplankton biomass during the mucilage event did not significantly differ from the

102   years without the event (Revelante and Gilmartin, 1991; Flander Putrle et al., 2000; Najdek et

103   al., 2002; Flander Putrle, 2003), it was suggested that macroaggregates development does not

104   influence the phytoplankton biomass in the surrounding water (Flander-Putrle and Malej,

105   2008).

106   For some phytoplankton species macroaggregates represent a highly favourable

107   microhabitat (Alldredge, 1976). *Cylindrotheca closterium* has been recognised as a recurrent,

108   opportunistic diatom, colonising regularly already formed macroaggregates (Najdek et al.,

109   2002; Totti et al., 2005). It seems that the macroaggregates, simulating nutrient rich and hard

110   bottom, represent an optimal habitat for this benthic species. After colonisation of a

111   macroaggregate (Najdek et al., 2002), follow an intense multiplication (Monti et al., 1995) and

112   a consequent dominance of *C. closterium* in the phytoplankton community, often ending with

113   monospecific populations (Najdek et al., 2002; Totti et al., 2005). This process was also

114   observed in the laboratory conditions (Kraus et al., 2004). Hence, according to the percentage

115   contribution of *C. closterium* in macroaggregates, it is feasible to deduce whether a

116   macroaggregate is a freshly formed one, an aging or aged one (Najdek et al., 2002; Blažina et

117   al., 2005; Totti et al., 2005). It appears that *C. closterium* has an enhanced potential of

118   reproduction in the mucous compared to other species and that it consequently prevails over all

119   other species initially inhabiting macroaggregates (Grossart, 1999; Degobbis et al., 1999). *C.*

120   *closterium* prolonged existence in mucilage macroaggregates may also be related to a persistent

121   nutrient input in macroaggregates, resulting from a continuous internal recycling of the organic

122   matter (Kaltenböck and Herndl, 1992; Decho and Herndl, 1995). This species is also known for

123   the lavishing exudation of mucilage matter (Monti et al., 1995; Alldredge, 1999), under

124   controlled stress conditions, such as nutrient starvation (Monti et al., 1994; Welker and Monti,

125   1994). Under the specific conditions of marked stratification and P-limitation, *C. closterium*

126   exudates are hypothesised to relevantly contribute to the accumulation and persistence of

127   organic matter in the region (Urbani et al., 2005).

128   Abrupt changes of the physical and biogeochemical conditions in the basin seem to

129   precede the development of mucilage event (Cozzi et al., 2004; De Lazzari et al., 2008; Blažina

130   et al., 2011). The event seems to start usually in the upper layer of the extremely stratified

131   seawater column (Alldredge and Crocker, 1995; Degobbis et al., 1999; Najdek et al., 2002;

132   Precali et al., 2005) when the waters of the NA are in restricted contact with waters of the central

133   Adriatic (Degobbis et al., 2000). The formation of a usual phytoplankton bloom in a circulation

134   system of the NA was already observed (Kraus and Supić, 2011). Macroaggregates are also

135   held to accumulate within the isolated circulation cells, in which freshened waters from the Po

136   River delta are kept for a longer time period, and whose position is well described by the

137   distribution of geostrophic currents (Supić et al., 2000; Supić et al., 2001-2; Supić et al., 2003).

138   Circulation patterns of the NA show the pronounced interannual variability (e.g., Supić et al.,

139   2012). In general, the region is included in the large Adriatic-wide cyclonic meander during

140   cold part of the year and gets separated from it in the warm part of the year, when several

141   circulation cells become well developed (Krajcar, 2003). A cyclonic gyre typically appears

142   north to the Po River delta and an anticyclonic in the eastern part off Rovinj. The anticyclonic

143   is identified by the presence of a current in the eastern coastal zone, the Istrian Coastal

144   Countercurrent (ICCC) which, according to Supić et al. (2003), was present in the entire period

145   from March to September of 1997. Once formed, the macroaggregates distribute over the entire

146   water column, with a tendency of accumulation around the pycnocline (Herndl, 1992; Alldredge

147   and Crocker, 1995). Throughout the extended residing period at the pycnocline layer, the

148   macroaggregates grow to larger forms (Precali et al., 2005). During the entire period of the

149   mucilage event, all types of macroaggregates continuously form (Najdek et al., 2005; Precali et

150   al, 2005). The small macroaggregates are paired with the large ones and it is supposed that they

151   form concurrently and/or that the small ones are torn from the large ones (Najdek et al., 2002).

152   Macroaggregates buoyancy changes induce their vertical movements. They gain

153   buoyancy from the numerous gas bubbles forming within, due to the constant inside

154   microbacterial processes, which enable them to float towards the surface (Rinaldi et al., 1995).

155   Correspondingly, the diffusion of more saline waters into macroaggregates induces their loss

156   of buoyancy, which is followed by their sinking (Alldredge and Crocker, 1995). Conversely to

157   macroaggregates vertical movements, their horizontal whereabouts remain rather unexplained.

158   The concept that macroaggregates occurred at an earlier time and/or at the different site from

159   their sampling location was already introduced (Revelante and Gilmartin, 1991). Yet, without

160   any conclusive evidences, the assumption that macroaggregates can be dispersed from their

161   origin by currents, remained only a hypothesis (Degobbis et al., 1995; Rinaldi et al., 1995;

162   Cataletto et al., 1996; Danovaro et al., 2009).

163   Turbulence induced by weak winds, resulting with mixing in upper layers, is

164   held to facilitate the aggregation processes (e.g., de Lazzari et al., 2008). On the other hand, in

165   conditions of several days blowing of the NE weak winds the large aggregates can be dispersed

166   and/or settled to the bottom (e.g., de Lazzari et al., 2008). Unusually persistent and intense wind

167 blowing, mainly bora, can regress or interrupt the phenomenon development (Russo et al.,
168 2005), while the storms were attributed to have interrupted the mucilage event (Russo et al.,
169 2005, Precali et al., 2005).

170   The aim of our work was to investigate the effects of the sea dynamics on the mucilage
171 event basing our research on 1997 data. This was done by analysis of the microphytoplankton
172 species composition in the macroaggregates and in surrounding waters, surface heat fluxes and
173 mixing in the water column and geostrophic currents.

174

175 ## 2.   MATERIALS AND METHODS

176 **2. 1. Data**

177   We analyzed three types of data obtained at the oceanographic cruises in the NA during
178 the summer and autumn of 1997: (a) phytoplankton data (128 seawater and 21 macroaggregate
179 samples, sampling dates in Suppl. 1. and Table 4, respectively), (b) oceanographic data
180 (temperature and salinity) and (c) meteorologic data and sea surface temperature data for
181 computing surface fluxes. Temperature, salinity and seawater phytoplankton samples were
182 collected during summer of 1997 in July (8, 22, 23 and 24), August (4, 11 and 12) and
183 September (1 and 23) at the standard depths (0 m, 5 m, 10 m, 20 m, 25 m and near the bottom,
184 approx. at 30 m) at nine stations in the NA (SJ001, SJ007, ZI012, SJ108, SJ101, SJ103, SJ105,
185 SJ107 and ZI032; Fig. 1.). Stations SJ105 and SJ107 are deeper (35 m), so at SJ105 bottom
186 layer was sampled at 35 m, however at SJ107, at 30 and 35 m. Oceanographic data were, during
187 the 22-24 July and 11-13 August cruises, sampled at several additional stations in the region
188 (Fig. 1.). To get a rough estimation of meteorological and hydrological conditions during and
189 between the cruises in July and August we used in addition wind data measured three times a
190 day at Pula station (at 6 h, 13 h and 20 h UTC) and data on the Po River daily discharge rates
191 collected at the station Pontelagoscuro. Wind data were supplied by the Hydrometeorological
192 Institute, Zagreb and by the "Assessorato della Programmazione, Pianificazione e Ambiente" of
193 the Emilia Romagna region (Italy).

194

195 **2.1.1.   Phytoplankton data**

196 **2.1.1.1.   Collection of samples and subsamples treatment**

197   Five litre seawater samples were collected with Van Dorn bottles, immediately filtrated
198   through 300 μm mesh plankton net and subsamples of 200 mL taken for phytoplankton
199   determination.

200   Mucilage macroaggregates were sampled by scuba divers at various depths (7, 9, 10, 11,
201   12, 15, 16, 18 and 20 m). Depending on the macroaggregate size, samples were taken by 500
202   mL Plexiglas tubes (diameter 5.5 cm) closed by a rubber stopper at both ends (large
203   macroaggregates, ranging approx. from 2 m to 5 m in length and from 0.5 m to 2 m in height)
204   or by 20 mL polyethylene syringes with the forward end cut off (small macroaggregates, flocks
205   of diameter up to 10 mm).

206   Subsamples of small macroaggregates (15 – 20 mL), large macroaggregates (20 – 200
207   mL) and seawater (200 mL) were immediately preserved with Lugol's solution prepared with
208   sodium acetate, stored at + 4 ˚C and processed within a month. Prior to microscopic analysis,
209   subsamples of macroaggregates were carefully shaken manually, to homogenize the sample,
210   yet to prevent the deformation of cells. In cases of high mucosity of a sample, which could
211   diminish the accuracy of cell count and determination, the sample was diluted with filtered
212   seawater.

213   **2.1.1.2.   Phytoplankton determination**

214   Phytoplankton abundance and composition were determined at 200 x magnification in
215   100 random vision fields (if necessary, 50, 200 or 400 depending on the sample density) after
216   40 hours sedimentation of a 50 mL subsample by a Zeiss inverted microscope, using the
217   Utermöhl settling technique (1958). In our analyses we used phytoplankton data in the size
218   range of 20 – 200 μm. Identification was carried out to the species or genus level.

219   **2.1.2.   Oceanographic data**

220   Temperature and salinity were used to assess surface geostrophic currents relative to the
221   30 dbar fields, which derive from spatial distribution of dynamic depths of the corresponding
222   surface. At each sampling station (s), for each separate cruise (c), the dynamic depths of the 30
223   dbar surface [$D_{30}(s,c)$-$D_0(s,c)$] were computed after:

224
$$D_{30}(s,c) - D_d(s,c) = \int_d^{30} \alpha(s,\ c)\ dp.$$

225   The specific volume α depends on sea density ρ and equals to α=1/ρ. Sea density was computed
226   from temperature and salinity data at standard depths using standard equation.

227   Each sampling station was, for each separate cruise, characterised with oceanographic

228   parameters (OP) which are thermocline depth (assessed from the data at the standard sampling

229   depths and amounting to 7.5 m, 15 m or 25 m), average temperature, salinity and density above

230   and below the thermocline, density differences between layers above and below the

231   thermocline, density differences between surface and 30 m layer, density differences between

232   surface and 20 m layer, dynamic depth of the 30 dbar surface and dynamic depth of the 20 dbar

233   surface.

234   2.1.3. Set of data for computing air-sea fluxes

235   The set of data consists of daily values of standard meteorological data (air pressure, air

236   temperature, wind speed, fractional cloud cover, water vapour pressure and precipitation)

237   measured at Pula Meteorological Station (44° 52' N, 13° 55' E; Fig. 1) and sea surface

238   temperature (SST) data, measured at the lighthouse Sv. Ivan na Pučini, in the interval from 1

239   July to 30 September 1997. These data were provided by the Hydrometeorological Institute in

240   Zagreb (meteorological data) and by the Maritime Meteorological Center in Split (sea surface

241   temperature data). Surface fluxes, among which we present the surface loss due to evaporation

242   Q_e and total heat air-sea heat flux Q, were computed using the standard set of equations proposed

243   by Gill, as described in details by Supić and Orlić (1999).

244   2. 2. Data analysis

245   For statistical analyses of phytoplankton dataset PRIMER (Plymouth Routines In

246   Multivariate Ecological Research) v5 software package was used. As a transformation method,

247   we used contribution percentages of each species in the sample, to enhance the importance of

248   qualitative and down–weight the quantitative aspect of the data, as the comparisons were

249   performed between seawater samples and macroaggregate samples, which considerably differ

250   in phytoplankton abundances.

251   Seawater phytoplankton dataset obtained during July and August 1997 was separated in

252   13 seawater phytoplankton groups (further in text: SPG) upon the cluster analysis (not shown).

253   Groups were formed at the similarity level of 60 and above. The significance of the spatial and

254   temporal variation between the SPGs obtained by a Cluster analysis was tested using a One–

255   Way Analysis of Similarities (ANOSIM) routine (Table 1b). Multivariate routine SIMPER

256   (similarity percentage) was used to calculate the average similarity percentage between at least

257   two samples, based on the overall percentage contribution of each species in the sample. In our

258   research, SIMPER was used to calculate similarities between the 13 determined SPGs (Table

259   1.a), within each SPG (Table 2.a) and between each of 21 macroaggregate samples and each of

260   13 SPGs (Table 4). The maximum similarity between the two samples (totally identical

261   samples) would equal 100, while no similarity would equal 0. SIMPER was also used to

262   quantify the overall species contributions to each SPG (Table 2a) and macroaggregate (Table

263   3). Similarities of 40 or higher were considered significant as they belong above upper quartile

264   of all calculated similarities.

265   We calculated basic statistics of OP for each separate cruise (8 July, 22-24 July and 11-

266   12 August; Suppl. 2) at stations of hypothetical macroaggregate formation (origin stations),

267   stations where macroaggregates were found (sampling stations), stations where

268   macroaggregates were supposed not to have been formed (non-origin stations) and complete

269   dataset (all stations).

270   Aditionally, sets of OP were, for each separate cruise (8 July, 22-24 July and 11-12

271   August; Table 6), were analysed by PCA to find out the main OP characterising the investigated

272   stations. Note that input parameters for the PCA were sets of OP with parameter Origin. Origin

273   is a parameter which resulted from our investigation on hypothetical locations of

274   macroaggregates formation. Stations where macroaggregate/s were assumed to have formed

275   was characteristised by 1, while stations where macroaggregate/s were assumed not to have

276   been formed were characteristised by 0. All OP data were log (X+1) transformed.

277   The Distance-based linear model (DISTLM) and distance-based redundancy analysis

278   (dbRDA) were used for determination of the relation between phytoplankton community at 0

279   m, 10 m or bottom and OP for each cruise separately (8 July, 22-24 July and 11-12 August;

280   Suppl. 3). Analyses were performed (a) with information on origin (Origin included) and (b)

281   without it (Origin excluded). For DISTLM we used Euclidean distance for creating the

282   resemblance measure, forward selection as procedure and adjusted R^2 as criterion.

283

3.   RESULTS

3.1.   Phytoplankton community in the NA during the summer of 1997

3.1.1. Seawater phytoplankton community

287   Table 2a represents 13 SPGs, outlined by similarities between the seawater phytoplankton

288   samples obtained in July and August of 1997, based on species percentage contributions to each

289   sample. After establishing the statistical significance of difference between the determined

290   SPGs with ANOSIM test (R= 0,967, significance level = 0,1 %), these SPGs were used in

291   further analyses in our work. Based on similarities between the SPGs, the association

292 schematics of SPGs was created (Fig. 2). Horizontal and vertical distributions of the seawater
293 phytoplankton community in the NA observed on 8 July, 22-24 July and 11-12 August 1997
294 are presented by means of determined SPGs in Fig. 3 and Fig. 4, respectively. In Table 2b we
295 present distribution of SPGs with dominant species during July and August at the sampled
296 stations and depths.

297 The situation in the NA on 8 July was rather complex (Figs. 7a,b and 8). The waters from
298 the Po River delta, after a huge Po River discharge accumulated in the two low salinity surface
299 pools, one around st. SJ108 and another one about st. SJ103 – st. SJ105. In both, SPG 2 with
300 dominant diatom *Skeletonema costatum* was observed. Additionally, this riverine discharge
301 induced a pronounced vertical gradient at st. SJ108, resulting in a stratified array of
302 phytoplankton communities (SPGs 1, 2, 8 and 12, with diverse dominant diatoms: *Chaetoceros*
303 *socialis*, *S. costatum*, *Leptocylindrus danicus* and *Pseudo-nitzschia delicatissima*, respectively).
304 At the surface layer at st. SJ101 and st. SJ107, SPG 9 with dominant *P. delicatissima* was
305 observed, which was an older water body according to the higher salinity at the locations. In
306 the lower layer at the eastern part, a higher salinity waters with SPG 12, dominated by *P.*
307 *delicatissima,* were spread between st. SJ101 and st. SJ107.

308 During the entire analysed period, diatoms dominated the NA microphytoplankton
309 community. Later in July (22–24), at the surface of st. SJ001, SJ101, SJ103 and SJ007, SPG 4
310 with *Dactyliosolen fragilissimus* was detected, while at the rest of the region SPGs 12 and 13
311 with *P. delicatissima* were observed. Only at the bottom at st. SJ001, SPG 7 with *Nitzschia*
312 *longissima* f. *tenuirostris* was found. On 11–12 August, *D. fragilissimus* was dominant species
313 at the surface layer of the entire region (SPGs 4 and 5). At the lower layer, *P. delicatissima* was
314 dominant (SPGs 10–13), with *Paralia sulcata*, *N. longissima* f. *tenuirostris* and *Cylindrotheca*
315 *closterium* found respectively at st. SJ107, SJ007 and ZI012 in SPGs 3, 7 and 6.

316 Due to specific importance of *Thalassionema nitzschioides* and *Cylindrotheca closterium*
317 during the 1997 mucilage event, we present vertical distribution of these two particular species
318 in the period from July to September (Fig. 5 and Fig. 6, respectively). On 8 July 1997, *T.*
319 *nitzschioides* was first noticed solely in the upper layer at st. SJ103. Over the following two
320 weeks, it spread over the entire water column of st. SJ103, westwards in the surface layer to st.
321 SJ101 and SJ108 and eastwards in the bottom layer to st. SJ105. Until mid August it was
322 detected over the entire water column of st. SJ103 and SJ105 and further eastwards, in the
323 surface layer of st. SJ107. In the beginning of September it was found in the upper 10 m at all
324 stations of the Po River–Rovinj profile (except at st. RV001) and spread over the entire water

325 column later in the month. Similarly, distribution of *C. closterium* on 8 July started from one

326 location, surface of st. SJ108. Later in the month, it was found additionally in the bottom layer

327 of st. SJ103. During mid August, it was detected from 10 m towards bottom of st. SJ103, SJ105

328 and SJ107. Over the next month, it spread over the entire Po River–Rovinj profile (except at st.

329 RV001), from 5 m depth towards bottom.

330 **3.1.2. Mucilage macroaggregates phytoplankton community**

331 List of all 21 sampled macroaggregates (10 large and 11 small ones) with sampling

332 location (station and depth) and date, and phytoplankton composition is presented in Table 3.

333 In Table 4 we present similarities between each macroaggregate and every SPG established

334 during the period 8 July – 11 August as well as the hypothetical time and location of formation

335 of each macroaggregate (i.e., origin water column). We hypothesized the most possible

336 formation location/s and point/s in time for each macroaggregate considering several factors:

337 similarities between the macroaggregate and SPGs (Table 4) and the distribution patterns of the

338 two species, *Thalassionema nitzschioides* (Fig. 5) and *Cylindrotheca closterium* (Fig. 6).

339 Macroaggregates that we believe have remained at the formation location until sampling are

340 referred to as "residing", while the ones which are supposed to have been transferred from the

341 hypothetical formation location to a different, sampling location are referred to as "transient"

342 macroaggregates.

343 **3.1.2.1. Macroaggregates sampled on 22-23 July**

344 *Residing macroaggregates* **(3, 4, 6, 7 and 8)**

345 Macroaggregates contained none or up to 18 % of *Cylindrotheca closterium*, indicating

346 that probably none or only some succession changes occurred inside them. Data suggest that

347 these macroaggregates most probably remained at the formation station, i.e., that the sampling

348 station is also the (hypothetical) formation station, as the highest similarities of these

349 macroaggregates (40 – 79 %) were with SPGs which were observed at the time of sampling at

350 the sampling station.

351 *Transient macroaggregates* **(1, 2 and 5)**

352 Macroaggregates contained from 14 up to 52 % of *C. closterium*, indicating that probably

353 some or even considerable succession changes occurred inside them. Generally, similarities

354 with all SPG's were low (< 30). However, presence of *Thalassionema nitzschioides* in all three

355 macroaggregates (13 – 67 %) implies that this diatom was obligatory present in the seawater

356 at the locations and during moments when they formed, or later passed during their transport

357 by currents, and that during that time some succession changes did occur. As this diatom was

358 detected only at st. SJ103 until 22 July, it is possible that these macroaggregates were formed

359 at this station, wherefrom they were transferred by currents to their sampling stations, st. SJ107

360 and st. SJ108.

361 **3.1.2.2. Macroaggregates sampled on 4 August**

362 Unfortunately, no microphytoplankton was determined in the seawater samples on this date.

363 *Resident or transient macroaggregates* **(11 and 12)**

364 Macroaggregates contained none and 18 % of *C. closterium*, indicating that probably

365 none or only some succession changes occurred inside them. Highest similarities of these two

366 macroaggregates was with SPG 4 (59 – 74 %), which was noticed to have spread with currents

367 from st. SJ101/SJ103 to almost the entire region during the period from 22–24 July until 11–12

368 August, indicating that this most probably occurred at st. ZI032 as well. Hence, we data suggest

369 these macroaggregates could have formed anywhere in the area during late July, that they went

370 through some succession changes and remained at/floated to st. ZI032 where they were

371 sampled.

372 *Transient macroaggregates* **(9 and 10)**

373 Both macroaggregates contained high abundances of *C. closterium* (66 – 75 %),

374 indicating occurrence of considerable succession changes. Moreover, *T. nitzschioides* was

375 detected in both macroaggregates (8 – 17 %) and *Nitzschia longissima* f. *tenuirostris* only in

376 the second one (8 %). A closest location where these diatoms were noticed was at the beginning

377 of July in the upper layer at st. SJ103, wherefrom it spread vertically towards bottom and

378 horizontally, westwards to st. SJ101 (5 m) and st. SJ108 (0 m) and eastwards to st. SJ105 (35

379 m) until 22 July. These data suggest that both macroaggregates formed in the area of st. SJ103

380 and floated to st. SJ107. Furthermore, as macroaggregate no. 9 comprised about 50 % more of

381 *C. closterium* and 50 % less of *T. nitzschioides* then macroaggregate no. 5, and since data

382 suggest that both macroaggregates originate from the same area (around st. SJ103), we suppose

383 that macroaggregate no. 9 is an aged "macroaggregate np. 5 – type", i.e., that macroaggregates

384 after formation at st. SJ103 in July, floated to st. SJ107 and went through succession changes

385 until 4 August.

386 **3.1.2.3. Macroaggregates sampled on 11-12 August**

387 *Residing macroaggregates* **(13, 14, 15, 16, 17 and 20)**

388   Macroaggregates contained various proportions of *C. closterium* (from none to 7 % and

389   88 %), indicating that none, some or even considerable succession changes occurred inside

390   them. All macroaggregates except no. 16 showed highest similarities with the SPG 4 (40 – 80

391   %) which was at the time detected over the surface layer of the entire Po River profile. Data

392   suggest that macroaggregates no. 13, 14 and 17 most probably remained at their formation

393   stations, st. SJ108 and st. SJ107, where they were sampled. Macroaggregate no. 15 formed at

394   the surface layer of st. SJ101 and sunk to 9 m depth where it was sampled. The no. 20 most

395   probably formed at st. SJ001 where no surrounding water was sampled, but most probably SPG

396   4 had spread also to this station (Fig. 3). The remaining no. 16 comprised of 88 % of *C.*

397   *closterium*, indicating substantial succession changes and resulting with low similarities with

398   any SPG. Hence, we based our conclusion on presence of 7,20 % of *T. nitzschioides* in the

399   macroaggregate. As *T. nitzschioides* on 22–24 July was observed at 5 m at st. SJ101 and at 0 m

400   at st. SJ103 in SPG 4, and at 10 m and 30 m at st. SJ103 in SPG 12, it seems that no. 16 also

401   remained in the same area in which it was formed, around st. SJ101– st. SJ103.

402   ***Transient macroaggregates*** **(19 and 21)**

403   Unfortunately, no microphytoplankton was determined in the seawater samples on this

404   date at the sampling stations of these two macroaggregates. Macroaggregate no. 19 contained

405   low proportion of *C. closterium* (4 %) and the other none, indicating scarce succession changes.

406   The first one comprised 78,80 % of *T. nitzschioides* which was found at the closest at 0 m at st.

407   SJ103 in late July and mid August and at 0 m in mid August at st. SJ105 in SPG 4, and at 10 m

408   at mid August at st. SJ105 in SPG 5. Hence, it is possible that these macroaggregates could

409   have formed there and circulating within a closed circulation cell got transferred to the sampling

410   location, st. SJ001. During that period some succession changes occurred. Macroaggregate no.

411   21 showed highest similarity with the SPG 4 (69,3 %), which was detected in the upper layer

412   of st. SJ007 on 11 August. Therefore, it is possible that it formed around st. SJ007 and was

413   transported to sampling location, st. ZI012.

414   ***Resident or transient macroaggregate*** **(18)**

415   This macroaggregate contained no *C. closterium*, however, as it contained high amount

416   of *T. nitzschioides* (63 %) we assume that some succession changes occurred within. Highest

417   similarities (38 – 40 %) were noticed with SPGs 4 and 5. In both SPGs this diatom was

418   observed. SPG 4 was detected at 5 m of the same station and SPG 5 at 10 m at st. SJ105, both

419   belonging to the same circulation system (Fig. 8). Hence, we suppose it could have formed at

420   either of the two stations.

421 **3.2. Wind data, Po River discharge rates and oceanographic conditions**

422   Daily values of the total surface heat fluxes in summer 1997 were highly dependent on
423 evaporative fluxes and wind speed (Fig. 7a). In July and August, as well as in the first part of
424 September, the total surface heat flux was generally positive with several episodes of surface
425 heat losses, among which the one on the 18 July was the most intense (above 200 W m^{-2}) and
426 followed by the ones on the 1 and 11 August, with surface heat losses of 160 W m^2 and 84 W
427 m^{-2}, respectively. After the 10 September, the sea was generally losing heat during an intense
428 heat loss episode (of 179 W m^{-2}), with maximal strength on 15 September (256 W m^{-2}). Wind
429 data taken at 07, 14 and 21 h (not shown) suggest that the most intense heat loss episode on 18
430 July was induced by wind from N in evening of the day, which was preceeded by winds from
431 W and followed by winds from WNW, that winds from ENE played an important role in
432 episodes of the 1 and 13 August and that winds from south induced the 27–28 August surface
433 heat loss episode. Po River rates were high only in the first half of July and were low and
434 constant afterwards (Fig. 7a).

435   According to hydrographic conditions, the water column across the Po River delta –
436 Rovinj profile on 8 July was stratified (Fig. 7), with minimal density values in the two low
437 salinity surface pools, one close to the delta at st. SJ108 (27) and another in the central part of
438 the profile around st. SJ103 (30). Two weeks later, on 22 July, a change in hydrographic
439 conditions was observed. The two lower density pools combined into one, extending from st.
440 SJ108 to around st. SJ105. Density increased with respect to the previous cruise, hence
441 documenting a strong mixing event after the 18 July surface heat loss episode. The common
442 feature of the horizontal distribution of dynamic depths of the 30 dbar surface on 22–24 July
443 and 11 August (Fig. 8) was the presence of the low salinity deep basin located south–east to
444 Rovinj, which was the central part of an anticyclonic gyre. However, in central and eastern part
445 of the investigated region different circulation patterns between the cruises were observed. On
446 22–24 July the motions in the western part of the Po River delta – Rovinj section were
447 anticyclonic, while on 11 August the transversal motions spreading waters from the Po River
448 delta towards east prevailed in the western and central part of the Po River delta – Rovinj
449 section.

450 **3.3. Environmental factors**

451   Simple statistics (Suppl. 1), cluster analysis (not shown) and PCA (Table 6) preformed
452 on datasets of 8 July, 22-24 July and 11-13 August 1997 showed that differences between areas

453   in which macroaggregates were formed (hypotheticaly, according to our analysis of similarity

454   between phytoplankton communities in macroaggregates and seawater) and other areas were

455   not highly pronounced. It seems that origin water columns were generally of lower salinity and

456   density in upper layers above the thermocline and were more stratified than surrounding areas

457   in which macroaggregates were not formed. Interestingly, results of PCA analysis indicate that

458   dynamic depths of origin columns were in July lower and in August higher than dynamic depths

459   of non-origin columns.

460   A much more detailed analysis was performed by DISTLM, which in addition to water

461   column parameters and information whether the water column was origin or non-origin one,

462   included seawater phytoplankton community composition. It showed that one particular SPG

463   can appear in various types of environmental conditions. The distribution of SPG's was mainly

464   driven by distribution of salinity and stratification degree and/or dynamic depths of 20 dbar

465   surface (Suppl. 2, Origin excluded). Similar as PCA, DISTLM pointed to salinity, density and

466   dynamic depths as the main environmental parameters which characterise the origin water

467   column. More specifically, it follows that macroaggregate formation, which as a rule occurs in

468   0 – 10 m layer, appeared in areas characterised by: (1) extremely low or high values of salinity

469   in the overall water column on 8 July, (2) low dynamic depths of 20 dbar surface, stratified

470   surface layer of 10 m and extreme low or high density values in the lower part of the water

471   column on 22–24 July and (3) high dynamic depths of 20 dbar surface, extreme values of

472   salinity in the overall water column and intensely stratification of the water column (Suppl. 2,

473   origin included).

474

475   4. DISCUSSION

476   *On locations of macroaggregates formation*

477   Although the mucilage formation was observed in the eastern Gulf of Trieste during May

478   1997 (Flander-Putrle and Malej, 2008), data suggest that massive mucilage event in the open

479   NA actually started after 8 July as during the cruise on that day no macroaggregates were found.

480   The first observed macroaggregates were found on 22–23 July (both large, no. 3 and 6, and

481   small, no. 7) in the layer 12 – 15 m at st. SJ001 and SJ101, locations belonging at that moment

482   to a cyclonic gyre (Fig. 8), and at 10 m at st. ZI012 (small, no. 8) to an anticyclonic one (Fig.

483   8). They had phytoplankton composition which was similar to the composition of the

484   surrounding water. Thus we conclude that they remained at their formation location until the

485   sampling, residing within a closed circulation cells of cyclonic or anticyclonic rotation sense.

486   There are more evidences that macroaggregates reside within gyres: the macroaggregate

487   no. 16, found on 11 August, according to *T. nitzschioides* distribution, formed previousely in

488   July around st. SJ101 – st. SJ103, and remained in the same area for a longer time period,

489   between the July and August cruises. According to our geostrophic circulation map, the

490   macroaggregate no. 16 was kept in a cyclonic gyre, present around st. SJ101 – st. SJ103 on both

491   22–24 July and 11 August cruises (Fig. 8). Interestingly, the basic of NA circulation patterns,

492   with an cyclonic gyre in western part of the region and anticyclonic in the eastern, as shown at

493   Fig. 8 for July and August cruises, remained (at least) till September, which is visible also on

494   one of the first satellite images of the NA taken on 16 and 17 September 1997 (Fig. 8; Mauri

495   and Poulain, 2001). It was already hypothesized that gyres are favourable location for

496   macroaggregate's formation and residing (e.g., Supić et al., 2001-2; 2003) and our findings

497   support these previous assumptions.

498   Our results show that during the entire mucilage event new macroaggregates are

499   constantly being formed and that at the same time in the same region old and fresh

500   macroaggregates coexist (as already observed by Precali et al., 2005 and Najdek et al., 2002).

501   Furthermore, data suggest that all macroaggregates during the 1997 mucilage event formed in

502   the upper layer (0 – 15 m), substantiating the thesis that the formation of mucilage

503   macroaggregates occurs predominantly above the pycnocline and in the upper layer (Degobbis

504   et al., 1995; Precali et al., 2005). In contrast, the sampling depths ranged from 7 to 20 m

505   indicating that some macroaggregates sink after the formation. These findings are in accordance

506   with the previous observations that macroaggregates during their life span sink to deeper layers,

507   usually accumulating around the pycnocline (Precali et al., 2005). We found no indication that

508   any of the macroaggregates rose in the water column after its formation during the 1997 event.

509   ***On the macroaggregates transport by geostrophic currents***

510   Several macroaggregates (no. 1, 2, 5, 9 and 10) seem to have formed at the st. SJ103, all

511   of them at the beginning of the 1997 mucilage event, as each macroaggregate contained

512   *Thalassionema nitzschioides*, a diatom which was at that time present only at this particular

513   location. These macroaggregates were sampled on 22 July and 4 August, both in the western

514   (at st. SJ108) and in the eastern part or the profile (at st. SJ107). Our idea that these

515   macroaggregates were transported by circulation pattern from around st. SJ103 to these two

516   sampling locations is sustained by the geostrophic currents patterns and velocities (Figs. 1 and

517   8). To reach these stations in three days the macroaggregate would travel with speed of 5 cm s^{-}

518   ^{1} (distance between st. SJ103 and st. SJ101 is around 13 km) or 10 cm s^{-1} (distance between st.

519   SJ103 and st. SJ107 is around 25 km). These values roughly coincide with speeds computed

520   for the alongshore section in eastern part of the region in summer 2003, and amounting up to 4

521   cm s^{-1} in calm conditions and up to 10 cm s^{-1} one day after an episode of surface heat loss (of

522   around 140 W m^{-2}) as presented by Lyons et al. (2007).

523   We assume that the circulation pattern observed on 22 – 24 July formed during the 18

524   July surface heat loss event, simultaneously with the changes in hydrographic conditions

525   discussed above in Results section. Thus, the macroaggregates formed and resided in a low

526   salinity surface pool at st. SJ103, before the surface loss of the 18 July event. After this date,

527   macroaggregates have likely been transported both towards east and west, as presented

528   schematically at Fig. 1, to st. SJ107 and st. SJ108. The idea that macroaggregates get transferred

529   from one location to another was already introduced (Franco and Michelato, 1992; Revelante

530   and Gilmartin, 1991; Cataletto et al., 1996; Russo et al., 2005; Danovaro et al., 2009). However,

531   in this work we investigated the idea more closely and found relation between macroaggreagate

532   and surrounding phytoplankton distribution and geostrophic circulation paths supporting this

533   idea.

534   ***On air-sea influence on phytoplankton species distribution and mucilage events***

535   Results of DISTLM analysis, relating salinity, and other parameters highly dependent on

536   it, density and depth of 20 dbar surface, to phytoplankton distribution, imply that mechanism

537   controlling the low salinity Po River waters spreading across the NA controls also distribution

538   of phytoplankton species in the investigated region. Spreading of Po River waters across the

539   NA is basically dependant on stratification degree, winds, and air-sea fluxes (e.g., Lyons et al.,

540   2007). The first heat loss episode, on 18 July, changed existing density fields and circulation

541   patterns, replaced the macroaggregates formed in central part of the Po River delta-Rovinj

542   profile towards east and west, and altered the existing phytoplankton distribution in the

543   investigated region. On 22-24 July cruise the number of SPG in upper layers was reduced with

544   respect to the 8 July cruise, and some SPG documented previously (e.g., 2, 8 and 9) totally

545   dissapered and were replaced by others (4, 12 and 13). The large expansion of low salinity

546   waters towards east between 22-24 July cruise and 11-13 August cruises brought SPG 4 (Figs.

547   3, 4 and 8), which seems to be the origin water of several macroaggreagates (Table 4). Thus,

548   SPG 4, residing in cyclonic gyre off Po River delta, was transported into the large anticyclonic

549   off Istra around st. SJ107, location at which before 22 July (Table 4) no macroaggregates were

550   formed. By introduction of new species with SPG 4, including the opportunistic *T.*

551   *nitzschioides*, the gyre around st. SJ107 became a new location of macroaggregates formation.

552   This explains the shift between July and August origin water columns position, which was

553 preferably in areas of low 20 dbar surface (cyclonic gyre) in July and in areas of high 20 dbar

554 surface (anticyclonic gyres) in August, as indicated by PCA (Table 6).

555 Spreading of lower salinity Po River waters after summer bora events up to the eastern coastal

556 zone and intensification of motions in the anticyclonic gyre off Rovinj, was previousely

557 documented (Lyons et al., 2007). Thus arrival of lower salinity waters with its specific SPG in

558 the eastern NA with shift in macroaggregate formation areas in 1997 seems to be provoked by

559 atmospheric forcing, namely by strong winds from ENE blowing during 1 August and/or 13

560 August surface heat loss episodes. The first and most intense surface loss episode of 18 July

561 was induced by N wind, which was preceeded by winds from W and followed by winds from

562 WNW, although changed significantly density fields and circulation patterns and transporting

563 around already formed macroaggregats, did not invoke lower salinity waters spreading to the

564 easten coast.

565   ***On*** *Cylindrotheca closterium* ***introduction in the water column***

566   The question of how a benthic diatom, *C. closterium*, occasionally detected in the water

567 column in the NA, enters the water column and subsequently colonises the macroaggregate, is

568 still unanswered (Monti et al., 1995; Alcoverro et al., 2000; Najdek et al., 2005; Totti et al,

569 2005). Resuspension and redistribution of microphytobentic species by water movements was

570 repeatedly reported (Thornton, 2002; de Jonge and Van Beusekom, 1992, 1995). We assumed

571 that this was the case with *C. closterium* and confirmed the assumption by analysing its

572 abundance in relation of oceanographic and meteorologic data.

573   At the beginning of the 1997 mucilage event, *C. closterium* was generally absent from

574 the investigated waters with the exception of surface layer at st. SJ108. The intense 18 July

575 evaporation event, which induced turbulent mixing in the entire water column, could have

576 provoked sediment resuspension and consequent *C. closterium* elevation from the sea bottom

577 into lower layers of the water column (as observed at st. SJ103; Fig. 6). It was previously

578 shown that the summer episodes of surface heat losses can reflect on dynamics of bottom layers

579 in the region, inducing bottom currents and changes in hydrographic conditions (e.g., Vilibić et

580 al., 2008). The intense episode on 18 July seems to be one of them. Namely, bottom salinity, at

581 all stations, increased for 0.5-0.6 (not shown). Such a large salinity rise is rarely observed

582 between the two subsequent cruises, as can be concluded from long term bottom salinity data

583 (at st. SJ107; Supić and Vilibić, 2006). Thus we believe that 18 July surface heat loss espisode

584 was capable of introducing mixing in the upper sediment layers, able to elevate bottom species

585 to upper parts of the water column, and induced *C. closterium,* which was absent previously

586 from deeper layers of the water column, as it was observed at 30 m depth at st. SJ103 on 22

587 July (Fig. 6). Other summer surface heat losses episodes, which occurred later, were less

588 intense, inducing thus also less intense near bottom turbulent mixing. Namely the bottom layer

589 density change (at 30 m) in the open NA (st. SJ101 – st. SJ107) was around 0.4 on 8 and 22

590 July and around only 0.04 between 11 August and 1 September. Thus these less intense surface

591 heat loss episodes were less effective in the bottom sediment elevation. (The rise in abundance

592 of opportunistic species as observed between 11 August and 1 September at Figs. 5 and 6 must

593 therefore be invoked by other reasons and not from sediment resuspension.)

594 Once *C. closterium* was elevated from sediment and was introduced in the water column,

595 it can easily reach and colonise existing macroaggregates.

596 ***On the opportunistic species*** *Thalassionema nitzschioides*

597 Just as *C. closterium*, *T. nitzschioides* is also a highly silicified, large pennate diatom,

598 favouring nutrient enriched habitats (Najdek et al., 2002). Our findings indicate that *T.*

599 *nitzschioides*, just as *C. closterium*, can prevail over other species inhabiting the

600 macroaggregates by multiplying to high abundances, regardless of the small initial abundance

601 of *T. nitzschioides* in the ambient seawater. Obviously, *T. nitzschioides* can successfully

602 outcompete other species in a macroaggregate just as successfully as *C. closterium* does.

603 Nevertheless, it seems that intense multiplication and dominance of *T. nitzschioides* in the

604 macroaggregate does not reduce the probability of the following, final succession phase

605 colonisation with *C. closterium* (see macroaggregate no. 9 in Results section). Consequently,

606 we can conclude that both, *C. closterium* and *T. nitzschioides* are opportunistic species of the

607 mucilage phenomenon. It is also interesting to notice that in one small macroaggregate (no. 8)

608 neither *C. closterium* nor *T. nitzschioides* were observed. This shows that for macroaggregate

609 formation, presence of the two opportunistic species is not essential.

610 Although 18 July heat loss episode induced sediment resuspension and elevation of *C.*

611 *closterium* in the water column, the same cannot be presumed also for *T. nitzschioides* as it was

612 already present in the upper layer of st. SJ103. Thus presence of *T. nitzschioides* in the bottom

613 layer of st. SJ103 on 22 July might have occurred alternatively, from vertical spreading from

614 the upper layer.

615 According to current state-of-the art, macroaggregate contains species which were

616 present in the water column at the time of its formation and later undergoes species succession

617 marked with colonisation and increase of *C. closterium* abundance, and microphytoplankton

618 diversity decrease and abundance reduction of all other species. Hence, it follows that *T.*

619 *nitzschioides* also entered macroaggregate during formation process. However, for our research

620   on macroaggregates transportation with currents it is irrelevant if the macroaggregate formed

621   or just passed a location with *T. nitzschioides.*

On the macroaggregate fractioning after the surface heat loss episode

623   Depending on the wind intensity, mucilage event can get interrupted or macroaggregates

624   dispersed without any major consequences on the event itself. The latter was the case which we

625   document with calculated surface fluxes. Phytoplankton composition indicates that the small

626   macroaggregate no. 4, found on 22 July at 10 m in SPG 12, was formed in SPG 9, i.e., in the

627   surface waters of the same location (st. SJ101) or nearby, around 8 July. Sampled

628   macroaggregate no. 4 was a small one. However, we are unsure whether this macroaggregate

629   was initially small or if it was originally part of a larger one which fractured. As between 8 and

630   22 July (on 18 July) an evaporation event occurred (Fig. 7), inducing turbulent mixing in the

631   water column, which could fraction a large, existing macroaggregate, the second hypothesis

632   seems to be more plausible. Presence of *C. closterium* in this macroaggregate (18 %) points out

633   that after its formation, some succession changes occurred inside this macroaggregate and thus

634   confirming that the macroaggregate could had been formed about two weeks earlier and was a

635   large one at the time.

On prolongation of macroaggregates life due to *Cylindrotheca closterium*

637   *C. closterium* exudates are hypothesised to relevantly contribute to the accumulation and

638   persistence of organic matter in the region under the specific conditions of marked stratification

639   and P-limitation (Urbani et al., 2005). As low P content and high C/P ratio were detected in

640   macroaggregates (Giani et al., 2005), it is possible that *C. closterium* exudates within the

641   macroaggregates might extend resident time of macroaggregates themselves.

On increased abundance of opportunistic species in the water column at the end of

643   ***mucilage event***

644   Less intense summer heat losses after 18 July did not induce so intense resuspension of

645   sediment as the one on 18 July. Thus the increased abundance of opportunistic species *C.*

646   *closterium* and *T. nitzschioides* came from another origin – which is, as we state here – from

647   the macroaggregates at time of their decay. This process explains the increase of their

648   abundance in the water column between 11–12 August and 1 September (Figs. 5 and 6). A

649   futher, large increase of abundances of *C. closterium* and *T. nitzschioides* during September, a

650   period following the 1997 mucilage event, originate from the macroaggregates from the

651   locations where they were present in large amounts. Intense turbulent mixing in water column

652   occurring during episodes of surface heat losses induced partial fragmentation and/or final

653 disintegration of macroaggregates during which species from the macroaggregates got released
654 into the ambient water.

655 ***On changes in abundance of the opportunistic species after the mucilage event***

656 Following the mucilage event, large abundances of opportunistic species remain in the
657 region where the event had occured. Thus pointing out that mucilage event can significantly
658 impact phytoplankton composition in the NA, particularly concearning the presence and
659 abundance of the opportunistic species.

660 ***On macroaggregates as vectors of microbial community over the marine realm***

661 "The mucilage can act as a controlling factor of microbial diversity across wide oceanic
662 regions and could have the potential to act as carrier of specific microorganisms, thereby
663 increasing the spread of pathogenic bacteria" (Danovaro et al., 2009). It is reasonable to add
664 that this applies to all microorganisms within the macroaggregates. Our investigation
665 substantiates this statement by presenting strong indications that geostrophic currents actually
666 do transport macroaggregates over wider areas. This implies that geostrophic transport of
667 marine snow as small, universally present macroaggregates, is an important mode of
668 transporting microorganisms to larger distances.

669

670 **5. CONCLUSIONS**

671 The hypothesis that microphytoplankton distribution is an useful tool in tracing
672 macroaggregates transport paths is confirmed with the existing circulation fields. The
673 macroaggregates get transported by the geostrophic currents and are most likely to appear in
674 the central part of gyres, in the upper layers. Surface heat losses during several bora (NE wind)
675 episodes at the beginning of August, close to the end of mucilage event, induced spreading of
676 lower salinity waters, in which macroaggregates formed, from western and central parts of NA
677 towards the east. These waters became part of an anticyclonic gyre which became in that way
678 a new area of macroaggregates formation.

679 *Thalassionema nitzschioides* is an opportunistic species of the mucilage phenomenon,
680 occurring occasionally (only if present in the water column during macroaggregate formation
681 or during transfer of macroaggregates by currents over their lifespan) and temporary in the
682 macroaggregate phytoplankton succession (followed by a succession climax with *C.*
683 *closterium*).

684 We documented that increased mixing in the water column after an evaporation event can
685 result with the increased abundances of the sediment origin species *Cylindrotheca closterium*
686 in the water column.

687 The species inhabiting the macroaggregates can influence the water community after their
688 release from the macroaggregates in the surrounding water due to partial fragmentation and/or
689 final disintegration of the macroaggregates.

690 The similar approach to the one applied here can be used in tracing plankton paths via
691 marine snow across the sea, also in other sea regions in which geostrophic currents play
692 significant role as it is case for NA. This could be especially convenient as the density data used
693 for computation of geostrophic current are easily available, and can be applied also for historic
694 data, as they are in standard measured during oceanographic cruises.

695

696 **FIGURES**

697 Fig. 1. Map of the NA with sampling stations and schematic of macroaggregates transport from

698 st. SJ103 towards st. SJ101 and st. SJ107, as indicated by geostrophic currents distribution on

699 21-24 July. Several stations at which only the OP data were taken are marked with black dots.
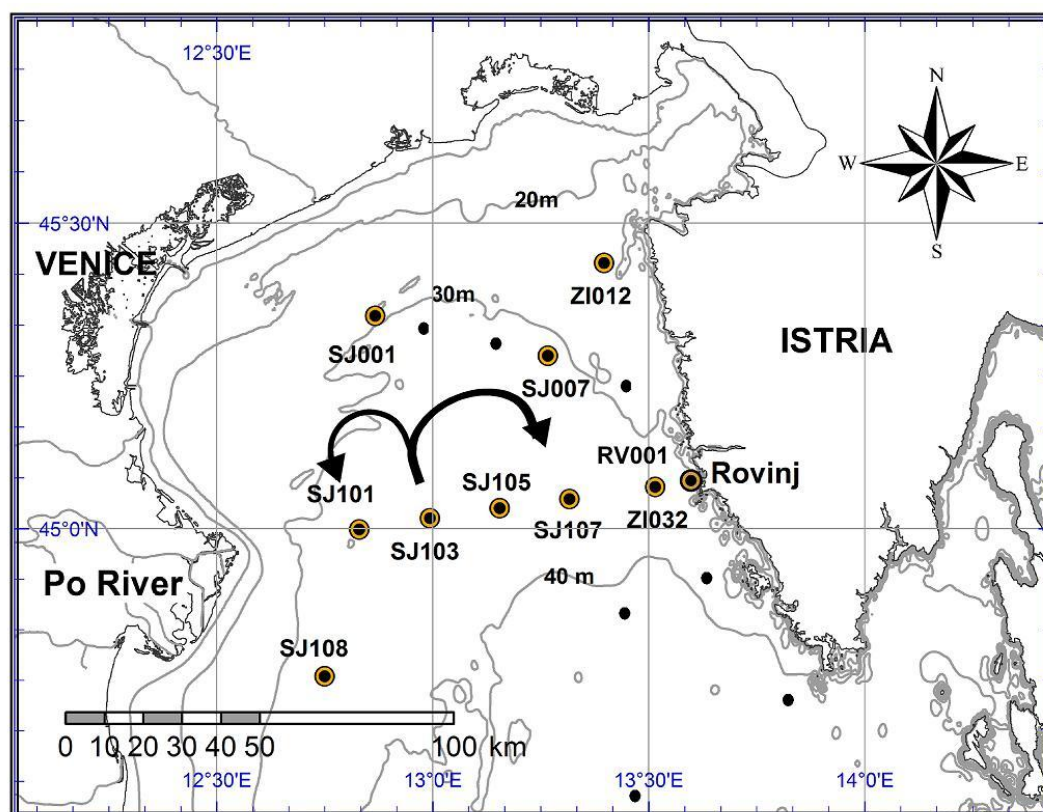

700

701 Table 1a. Average similarities between the 13 seawater phytoplankton groups (SPGs)

702 calculated by SIMPER multivariate routine. Similarities of 40 and higher are considered

703 significant as they belong above upper quartile of all calculated similarities (in bold on grey).

704 Statistical significance of SPGs were tested with ANOSIM (Table 1b).

705

	1	2	3	4	5	6	7	8	9	10	11	12	13
1													
2	**54**												
3	21	24											
4	11	17	26										
5	4	11	17	**52**									
6	9	15	28	21	23								
7	18	21	26	25	27	**54**							
8	**53**	**56**	24	16	17	14	20						
9	31	35	29	23	21	16	27	**56**					
10	26	20	**41**	20	17	27	24	19	**40**				
11	23	23	32	28	28	37	**54**	24	**43**	**59**			
12	26	24	26	21	16	20	30	27	**54**	**45**	**47**		
13	23	26	32	**49**	39	30	**40**	25	**51**	**47**	**56**	**53**	

706

707 Table 1b. Statistical significance of SPGs tested with ANOSIM. Bold on grey - statistically

708 significant results (p < 5%); On white - statistical significance unreliable due to unsufficient

709 size of one or both groups included in analysis; "—" - Pairwise tests failed (at least one group

710 must be larger than 1 in size). Size of groups presented in Table 3a.

711

	1	2	3	4	5	6	7	8	9	10	11	12	13
1													
2	0,96												
3	—	1											
4	**1**	**1**	**1**										
5	1	**1**	1	**0,98**									
6	—	1	—	**1**	1								
7	1	**1**	1	**1**	1	1							
8	1	**0,94**	1	**1**	1	1	1						
9	1	**1**	1	**1**	**1**	1	**1**	**1**					
10	—	1	—	**1**	1	—	1	1	1				
11	—	1	—	**1**	1	—	1	1	1	—			
12	**1**	**1**	**1**	**1**	**1**	**1**	**1**	**1**	**0,90**	**0,99**	**0,98**		
13	1	**1**	1	**0,92**	**1**	1	**0,96**	**1**	**0,92**	0,98	0,82	**0,88**	

712

713 Fig. 2. Association schematics of seawater phytoplankton groups (SPGs) based on significant

714 similarities between the SPG (complete presentation of similarities in Table 2). Full line

715 encircles five groups of SPGs based on presented similarities. Dashed line encircles SPGs in

716 which macroaggregates were hypothetically formed.
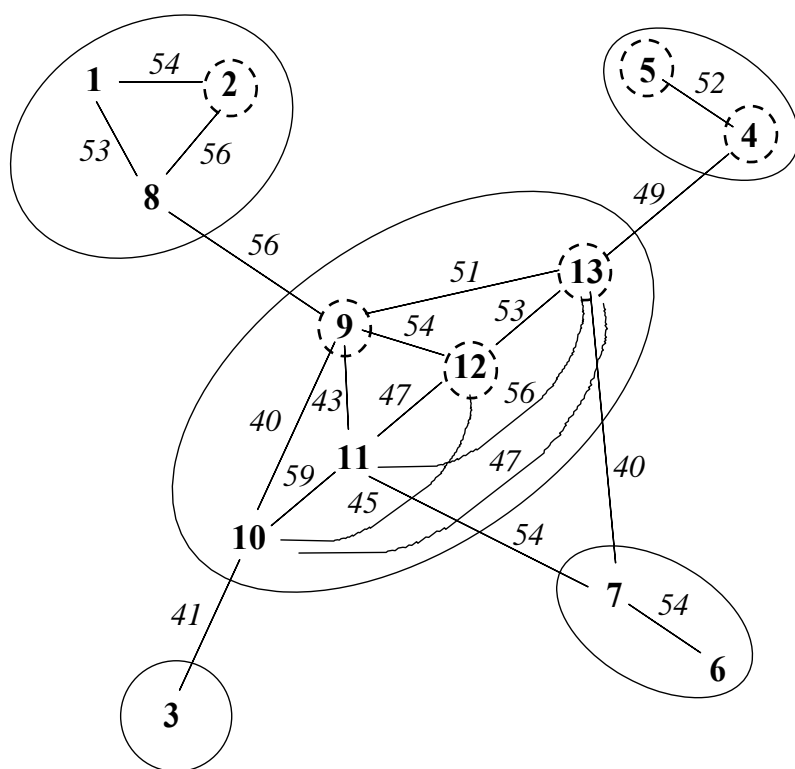
717

718

719 Table 2a. Phytoplankton community composition presented by average species contribution percentages and average similarity of 13 seawater phytoplankton groups (SPGs) calculated by SIMPER multivariate routine

720 (in bold - highest species percentage contribution for each SPG). * For SPG consisting of one seawater sample similarity is impossible to calculate.

	Average contributions of species / %												
SPG	1	2	3	4	5	6	7	8	9	10	11	12	13
Species													
Bacillariophyceae													
Cerataulina pelagica (Cleve) Hendey	0	2,69	12,00	13,62	0	0	0	3,55	6,00	0	0	1,49	8,26
Chaetoceros affinis Lauder	0	0,03	0	0,01	<0,01	0	0	<0,01	0,37	0	0	0,03	0,20
Chaetoceros curvisetus Cleve	0	0,06	0	0	0	0	0	<0,01	0,11	0	0	0,04	0
Chaetoceros insignis Pr.-Lavr.	0	0	0	0	0	0	0	0	0	0	0	<0,01	<0,01
Chaetoceros peruvianus Brightwell	0	0	0	0	0	0	0	0	0	0	0	0,01	0
Chaetoceros socialis Lauder	**43,62**	9,56	0	<0,01	0	0	0	9,48	3	0	0	<0,01	0,04
Chaetoceros sp.	0	<0,01	0	<0,01	<0,01	0	0	<0,01	0,25	0	0	0,01	0
Cylindrotheca closterium (Ehrenberg) Reimann et	0	<0,01	4,00	<0,01	<0,01	**40,38**	0	0	0	0	0	0,03	0,01
Dactyliosolen fragilissimus (Bergon) Hasle	1,06	1,65	8,00	**76,95**	67,27	11,54	9,53	4,06	5,31	4,76	12,82	5,65	35,57
Diploneis sp.	0	0	0	0	0	0	0	0	0	4,76	0	0	0
Guinardia flaccida (Castracane) Peragallo	0	0,03	4,00	0,10	0	0	2,30	0,20	0,14	4,76	10,26	1,21	1,82
Leptocylindrus danicus Cleve	0	4,31	4,00	<0,01	<0,01	0	0	**35,82**	24	0	0	0,53	0,10
Leptocylindrus mediterraneus (Peragallo) Hasle	0	0	0	0	0	0	<0,01	0	<0,01	0	0	0,01	0
Leptocylindrus sp.	0	0	0	<0,01	<0,01	0	0	0	0	0	0	<0,01	0,02
Navicula sp.	3,19	0,02	12,00	<0,01	0	0	0	0	0	14,29	0	0,14	<0,01
Nitzschia longissima f. *tenuirostris* Mereschowsky	0	0,98	8,00	1,22	<0,01	32,69	**55,28**	0,22	<0,01	14,29	17,95	1,44	3,87
Paralia sulcata (Ehrenberg) Cleve	7,45	<0,01	**28,00**	0	0	0	0	0	0	0	0	0,02	0
Pseudo-nitzschia delicatissima (Cleve) Heiden	21,28	17,11	8,00	5,77	<0,01	7,69	19,06	16,04	**49,93**	33,33	30,77	**86,10**	**46,62**
Pseudo-nitzschia seriata (Cleve) Peragallo	0	0	0	0	0	0	0	0	0	9,52	0	0,01	0
Rhizosolenia alata f. *gracillima* (Cleve) Grunow	1,06	0,48	4,00	0,09	1,82	0	0	3,41	4,26	0	5,13	1,93	0,74
Rhizosolenia sp.	0	0	4,00	<0,01	<0,01	0	0	0	0	4,76	0	0,08	0,02
Skeletonema costatum (Greville) Cleve	22,34	**62,87**	0	<0,01	0	0	0	26,33	2,76	0	0	0,12	<0,01
Thalassionema nitzschioides (Grunow) Hüstedt	0	0	0	0,17	3,64	0	<0,01	0	0	4,76	0	0,01	0,03
Bacillariophyceae (other)	0	0,04	0	0,07	1,82	1,92	<0,01	0,80	3,60	0	0	0,32	0,24
Dinophyceae													
Ceratium fusus (Ehrenberg) Dujardin	0	0	0	<0,01	<0,01	0	0	<0,01	0	0	12,82	0,03	0,02
Ceratium sp.	0	0,01	0	0,01	<0,01	0	0	0	0,04	0	2,56	0,01	0,04
Gymnodinium sp.	0	<0,01	0	0,52	3,64	1,92	9,21	0	0	0	0	0,09	0,25
Gyrodinium sp.	0	0,02	0	0,04	3,64	3,85	<0,01	<0,01	0	0	0	0,18	0,53
Protoperidinium sp.	0	0,06	4,00	0,01	0	0	<0,01	<0,01	0	0	0	0,05	<0,01
Dinophyceae (other)	0	0,06	0	1,35	18,18	0	4,61	0,10	0,32	4,76	7,69	0,47	1,32
Haptophyceae													
Syracosphaera pulchra Lohmann	0	0	0	0,07	0	0	0	0	0	0	0	<0,01	0,25
Haptophyceae (other)	0	<0,01	0	0	0	0	0	0	0	0	0	<0,01	0,02

Kraus, Romina; Supić, Nastjenjka (2015) *Sea dynamics impacts on the macroaggregates: a case study of the 1997 mucilage event in the northern Adriatic.* Progress in Oceanography, 138 (A). pp. 249-267. (preprint version)

AVERAGE SPG SIMILARITY	*	74	*	78	61	*	72	85	76	*	*	76	70
No. of seawater samples in each SPG	1	6	1	21	2	1	2	2	5	1	1	31	15

721

722 Table 2b. Dominant phytoplankton species in the seawater phytoplankton groups (SPG) determined on 8 July, 22/23 July and 11/12 August at the sampling
723 stations and
724 depths.

STATION	Depth/m	8 July		22-23 July		11-12 August	
		SPG	Dominant sp.	SPG	Dominant sp.	SPG	Dominant sp.
SJ108	0	2	*S. costatum*	13	*P. delicatissima*	4	*D. fragilissimus*
	5	12	*P. delicatissima*	12	*P. delicatissima*	4	*D. fragilissimus*
	10	8	*L. danicus*	12	*P. delicatissima*	4	*D. fragilissimus*
	20	2	*S. costatum*	12	*P. delicatissima*	13	*P. delicatissima*
	30	1	*C. socialis*	12	*P. delicatissima*	4	*D. fragilissimus*
SJ101	0	9	*P. delicatissima*	4	*D. fragilissimus*	4	*D. fragilissimus*
	5	8	*L. danicus*	4	*D. fragilissimus*	4	*D. fragilissimus*
	10	9	*P. delicatissima*	12	*P. delicatissima*	13	*P. delicatissima*
	20	2	*S. costatum*	12	*P. delicatissima*	12	*P. delicatissima*
	30	12	*P. delicatissima*	12	*P. delicatissima*	13	*P. delicatissima*
SJ103	0	2	*S. costatum*	4	*D. fragilissimus*	4	*D. fragilissimus*
	10	12	*P. delicatissima*	12	*P. delicatissima*	13	*P. delicatissima*
	30	2	*S. costatum*	12	*P. delicatissima*	13	*P. delicatissima*
SJ105	0	2	*S. costatum*	13	*P. delicatissima*	4	*D. fragilissimus*
	10	12	*P. delicatissima*	12	*P. delicatissima*	5	*D. fragilissimus*
	30	12	*P. delicatissima*	12	*P. delicatissima*	10	*P. delicatissima*
SJ107	0	9	*P. delicatissima*	13	*P. delicatissima*	4	*D. fragilissimus*
	5	9	*P. delicatissima*	12	*P. delicatissima*	4	*D. fragilissimus*
	10	9	*P. delicatissima*	12	*P. delicatissima*	4	*D. fragilissimus*
	20	12	*P. delicatissima*	12	*P. delicatissima*	11	*P. delicatissima*
	30	-	-	-	-	3	*P. sulcata*
	35	12	*P. delicatissima*	13	*P. delicatissima*	12	*P. delicatissima*
ZI032	0	-	-	13	*P. delicatissima*	-	-
	10	-	-	13	*P. delicatissima*	-	-
	30	-	-	13	*P. delicatissima*	-	-
SJ001	0	-	-	4	*D. fragilissimus*	-	-
	10	-	-	12	*P. delicatissima*	-	-
	30	-	-	7	*N. tenuirostris*	-	-
SJ007	0	-	-	4	*D. fragilissimus*	4	*D. fragilissimus*
	10	-	-	12	*P. delicatissima*	4	*D. fragilissimus*
	30	-	-	12	*P. delicatissima*	7	*N. tenuirostris*
ZI012	0	-	-	13	*P. delicatissima*	5	*D. fragilissimus*
	10	-	-	13	*P. delicatissima*	13	*P. delicatissima*
	30	-	-	13	*P. delicatissima*	6	*C. closterium*

727   Fig. 3. Horizontal distribution of seawater phytoplankton groups (SPGs) in the NA at 0 m, 10 m and 30 m (i.e., bottom) on 8 July, 22–24 July
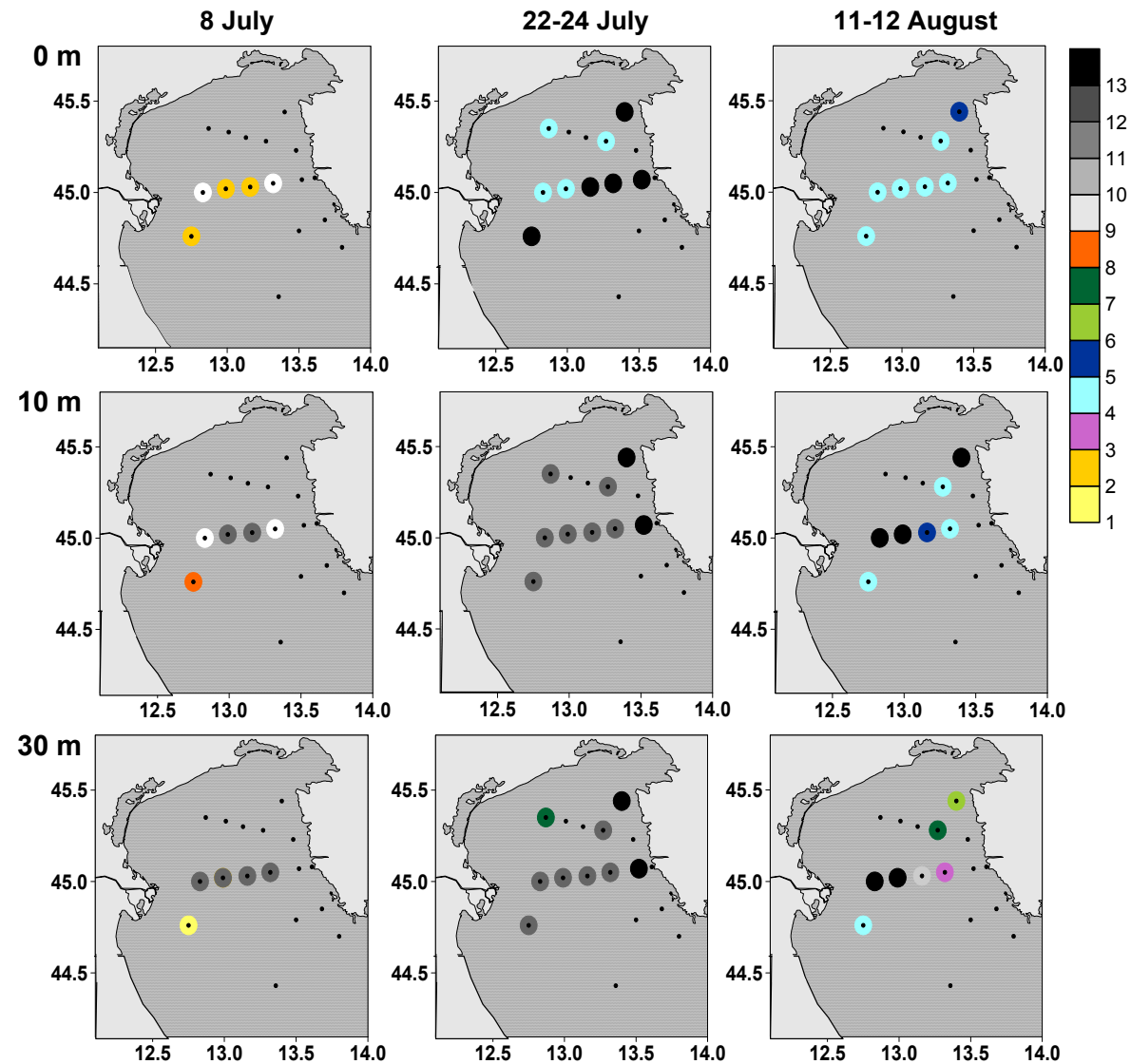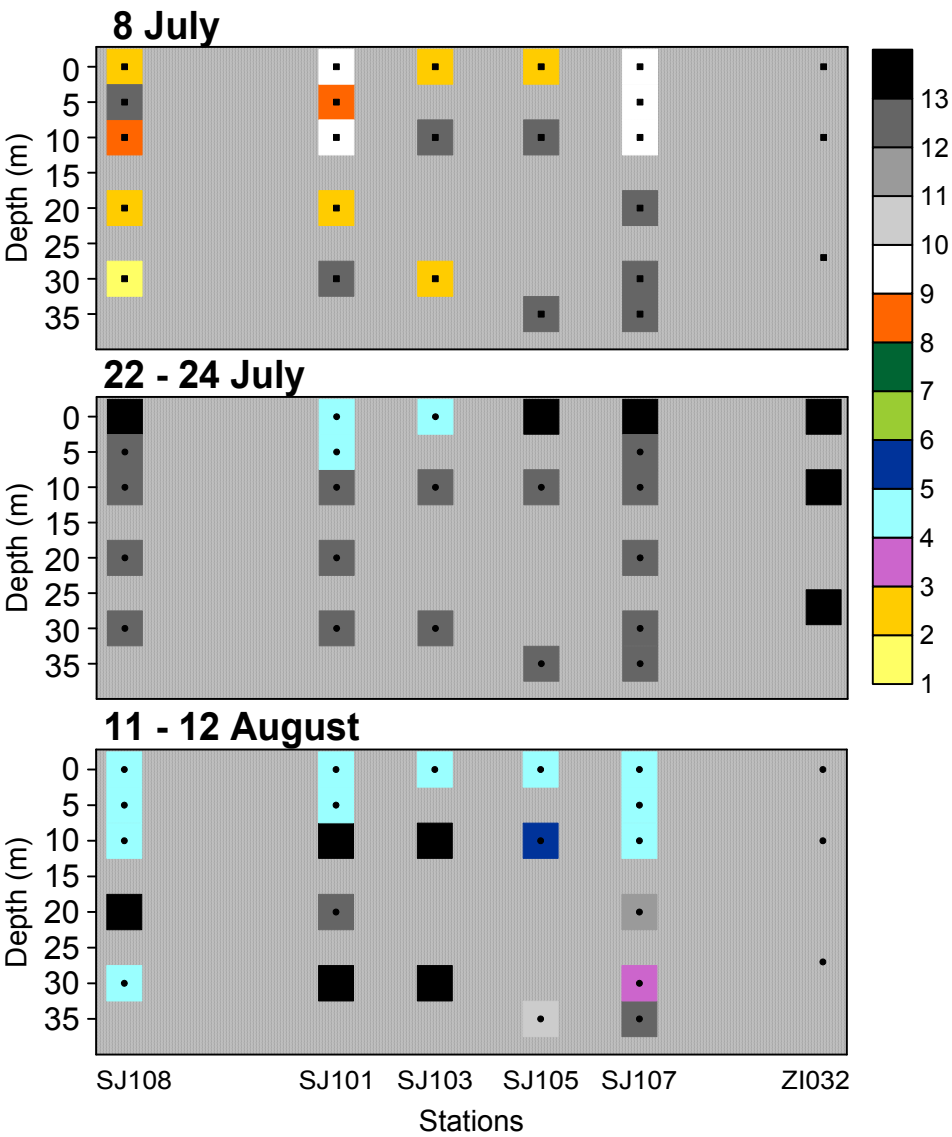728   and 11–12 August.

729   Fig. 4. Vertical distribution of seawater phytoplankton groups (SPGs) at the Po River delta – Rovinj

730   profile at 0 m, 5 m, 10 m, 20 m, 30 m and 35 m on 8 July, 22–24 July and 11–12 August.

731

732

733

758 Table 3. Macroaggregates phytoplankton community composition presented by species contribution percentages with information about

759 macroaggregates dimension and sampling location (date, station and depth). L – large, S – small macroaggregates.

Date	22 July 2012					23 July 2012			04 August 2012				11 August 2012						12 August 2012		
Macroaggregate / No.	1	2	3	4	5	6	7	8	9	10	11	12	13	14	15	16	17	18	19	20	21
Dimension	L	S	L	S	L	L	S	S	L	S	S	L	L	S	S	L	S	L	L	S	S
Station	SJ108		SJ101		SJ107	SJ001		ZI012	SJ107		ZI032		SJ108		SJ101		SJ107		SJ001		ZI012
Depth / m	11	11	12	12	16	15	15	10	10	10	7	18	12	12	9	15	10	20	20	12	10
Species																					
Bacillariophyceae																					
Cerataulina pelagica	2,72	1,46	2,64	0	0	4,51	2,00	4,08	0	0	39,14	17,91	16,79	29,58	21,21	0,49	45,25	0	0	47,62	0
Chaetoceros affinis	0,65	0	0	0	0	0	0	27,21	0	0	0	0	0	0	0	0	2,28	0	0	0	0
Chaetoceros socialis	0	0	0	0	0	1,20	0	0	0	0	0	0	0	0	0	0	0	0	0	0	0
Cylindrotheca closterium	51,59	15,20	4,34	17,91	13,66	2,67	0	0	66,03	75,36	0	11,55	6,96	1,41	0	87,46	1,90	0	4,40	0	0
Dactyliosolen fragilissimus	11,41	0	8,30	0	1,12	2,39	5,05	36,05	1,03	2,90	35,68	53,03	50,71	47,89	62,10	0,93	19,39	36,90	5,60	23,81	85,29
Guinardia flaccida	0	0	0,94	0	1,94	0	1,47	0,68	5,00	5,07	0,43	1,57	0,09	0	0,36	0	0	0	1,60	4,76	2,94
Guinardia striata	0	0	0,85	0	0	0	0	0	0	0	0	0,39	0	0	0	0	0	0	0	0	0,98
Leptocylindrus danicus	0	0	0,75	8,21	0,92	0	0	1,36	0	0	10,50	0	0	0	0	0	0	0	0	14,29	0
Leptocylindrus mediterraneus	0	0	0,38	0	0	0	0	0	0	0	0	0	0	0	0	0	0	0	0	0	0
Nitzschia longissima f. *tenuirostris*	0	0	2,26	1,49	0	1,57	0	0	0	7,97	0	0	10,80	12,68	9,43	2,16	25,48	0	0	0	0
Pleurosigma normanii	0	0	0	0	0,10	0	0	0	0	0	0	0	0,36	0	0	0	0	0	0	0	0
Pleurosigma sp.	0	0	0	0	0,20	0	0	0	0	0	0	0	0,18	0	0	0,05	0	0	0	0	0
Pseudo-nitzschia delicatissima	14,52	14,33	63,87	27,61	9,89	54,05	83,26	20,41	1,47	0	12,66	10,96	0,98	1,41	1,18	1,37	0,76	0	0	0	4,90
Rhizosolenia alata f. *gracillima*	5,70	0	3,11	6,72	0,61	1,93	0,74	2,04	4,12	2,17	0	0,49	0,18	0	0	0	0	0	0	0	1,96
Rhizosolenia sp.	0	0,29	0,09	0	0	0	0	0	5,00	1,45	0	0,39	0	0	0	0	0	0	0	0	0
Thalassionema nitzschioides	13,35	65,64	11,89	38,06	67,18	27,44	6,21	0	17,35	2,90	1,15	2,54	11,52	5,63	2,81	7,20	4,18	62,88	78,80	9,52	3,92
Bacillariophyceae (other)	0	0	0,09	0	1,63	3,41	0	6,80	0	0	0,29	0,68	0	0	0	0,29	0	0	0,40	0	0
Dinophyceae																					
Ceratium sp.	0	0,15	0	0	0,10	0,09	0,32	0	0	0	0	0	0	0	0,09	0	0	0,22	0,40	0	0
Gymnodinium sp.	0	0,44	0	0	0,41	0	0	0	0	0	0	0	0,54	0	2,54	0	0	0	0	0	0
Protoperidinium sp.	0	0	0,19	0	0,71	0	0,32	0	0	0	0	0,10	0	0	0	0	0	0	2,80	0	0
Dinophyceae (other)	0	2,49	0,28	0	1,53	0,74	0,63	1,36	0	2,17	0,14	0,39	0,71	1,41	0,27	0,05	0,76	0	6,00	0	0
Haptophyceae																					
Syracosphaera pulchra	0	0	0	0	0	0	0	0	0	0	0	0	0,18	0	0	0	0	0	0	0	0

760

761

762 Table 4. Summarised presentation of macroaggregates information: actual sampling and hypothetical formation locations and times, hypothetical

763 types of macroaggregates and macroaggregates movement path after the formation and calculated similarities by SIMPER routine between each

764 macroaggregate and determined seawater phytoplankton group (SPG) in the investigated area of the NA during the investigation period, July and

765 August of 1997. Abbreviations indicate as follows; types of macroaggregates: R (residing), T (transient), R / T (either resident or transient) and

766 macroaggregates movements: S (sinking), F (floating), none (no movement), none / F (none or floating). In bold on grey – high similarity of

767 macroaggregate sample with SPG indicates noted SPG as the formation location of a particular macroaggregate. In bold with frame – assumption

768 that noted SPG is the formation location based on *T. nitzschioides* presence both in macroaggregate sample and in water sample at the specific

769 depth and station.

NEW No.	ACTUAL DATA — Date, station and depth of macroaggregate sampling	HYPOTETICAL DATA — Date, station and depth of macroaggregate formation	Type of macroaggregate	Movement of macroaggregate after the formation	Similarity between macroaggregate and SPG												
					1	2	3	4	5	6	7	8	9	10	11	12	13
1	22 July, SJ108, 11 m	8 July, SJ103, 0–10 m	T	F	16,6	**20,1**	26,7	22,3	19,7	59,5	25,0	26,1	27,2	24,0	31,1	**25,7**	30,8
2	22 July, SJ108, 11 m	after 8 July, SJ103, 0–10 m	T	F	14,3	**14,9**	13,8	11,1	8,8	23,3	18,7	15,5	16,4	21,9	17,0	**17,1**	18,2
3	22 July, SJ101, 12 m	22 July, SJ101, 5–10 m	R	S	23,4	23,3	30,0	**22,7**	18,0	22,7	30,0	26,5	54,1	46,4	45,7	73,9	53,1
4	22 July, SJ101, 12 m	8 July, SJ101, 0–10 m	R	S	22,3	21,0	21,5	11,2	12,7	27,1	20,1	27,7	40,6	33,9	34,2	33,1	31,0
5	22 July, SJ107, 16 m	8 July, SJ103, 0–10 m	T	F	11,6	**13,2**	17,3	9,9	11,2	24,5	17,3	13,9	14,8	19,2	15,2	**15,3**	15,7
6	23 July, SJ001, 15 m	23 July, SJ001, 10 m	R	none	24,6	22,8	21,1	18,4	13,4	16,3	25,0	24,6	54,3	42,8	37,5	61,9	48,4
7	23 July, SJ001, 15 m	23 July, SJ001, 10 m	R	none	23,1	19,7	17,6	17,9	11,6	12,7	25,8	21,7	49,1	45,0	39,0	78,5	47,4
8	23 July, ZI012, 10 m	23 July, ZI012, 10m	R	none	22,5	24,4	24,2	50,5	52,0	21,2	30,7	27,3	39,2	27,2	37,3	34,1	57,4
9	4 August, SJ107, 10 m	8 July, SJ103, 0–10 m	T	F	3,6	**3,2**	18,5	3,8	8,0	42,9	7,6	6,2	6,2	16,8	11,6	**7,4**	7,2
10	4 August, SJ107, 10 m	July, SJ103	T	F	2,1	**5,3**	22,5	8,2	12,1	51,3	17,9	5,8	7,2	22,2	20,3	**10,4**	12,3
11	4 August, ZI032, 7 m	after 22 July, SJ107, 5–10 m or 22 July, ZI032, 10 m	R / T	none / F	13,7	25,4	32,4	**59,1**	44,7	19,5	23,2	31,7	36,5	19,2	26,1	24,8	51,0
12	4 August, ZI032, 18 m	after 22 July, SJ107, 5–10 m or 22 July, ZI032, 10 m	R / T	none / F	12,5	20,0	34,5	**73,9**	51,6	31,5	23,8	20,4	25,4	20,6	26,2	23,4	51,8
13	11 August, SJ108, 12 m	11 August, SJ108, 0–5 m	R	S	2,2	12,5	33,3	**69,0**	51,9	30,8	24,1	9,8	15,6	22,1	25,6	15,3	45,5
14	11 August, SJ108, 12 m	11 August, SJ108, 10 m	R	none	2,5	12,7	30,8	**69,9**	51,7	27,0	26,5	9,9	15,9	25,0	28,3	15,5	46,2
15	11 August, SJ101, 9 m	11 August, SJ101, 0 m	R	none	2,2	12,4	29,5	**80,6**	52,2	24,1	24,5	9,9	15,6	18,8	24,2	14,8	44,8
16	11 August, SJ101, 15 m	22 July, SJ101, 5 m or SJ103, 0–10 m	R	S	2,3	4,0	9,0	**4,5**	6,4	45,1	6,4	3,6	3,5	9,3	4,5	**4,5**	**5,1**
17	11 August, SJ107, 10 m	11 August, SJ107, 10 m	R	none	1,8	12,1	30,7	**40,6**	26,8	39,7	38,0	9,4	16,0	24,8	32,3	15,2	38,2
18	11 August, SJ107, 20 m	11 August, SJ107, 5 m or SJ105, 10 m	R / T	none / F	1,1	3,9	8,0	**37,5**	**39,8**	11,5	11,0	4,9	6,0	9,5	13,0	7,5	29,1
19	12 August, SJ001, 20 m	11 August, SJ105, 10 m	T	F	1,1	3,5	14,0	8,6	**15,6**	10,4	12,5	5,2	6,0	15,9	13,6	7,6	9,8
20	12 August, SJ001, 12 m	after 23 July, SJ001, 0 m	R	S	1,1	13,5	28,0	**40,6**	32,8	11,5	14,2	22,5	27,3	14,3	17,6	13,4	34,7

| 21 | 12 August, ZI012, 10 m | 12 August, SJ007, 0m | T | F | 7,0 | 9,7 | 17,8 | **69,3** | 51,3 | 16,4 | 18,2 | 11,9 | 13,1 | 16,5 | 22,6 | 15,4 | 37,5 |

770

Fig. 5. Vertical distribution of *Thalassionema nitzschioides* at the Po River delta – Rovinj profile on 8 July, 22–24 July, 11–12 August, 1 September and 23 September.
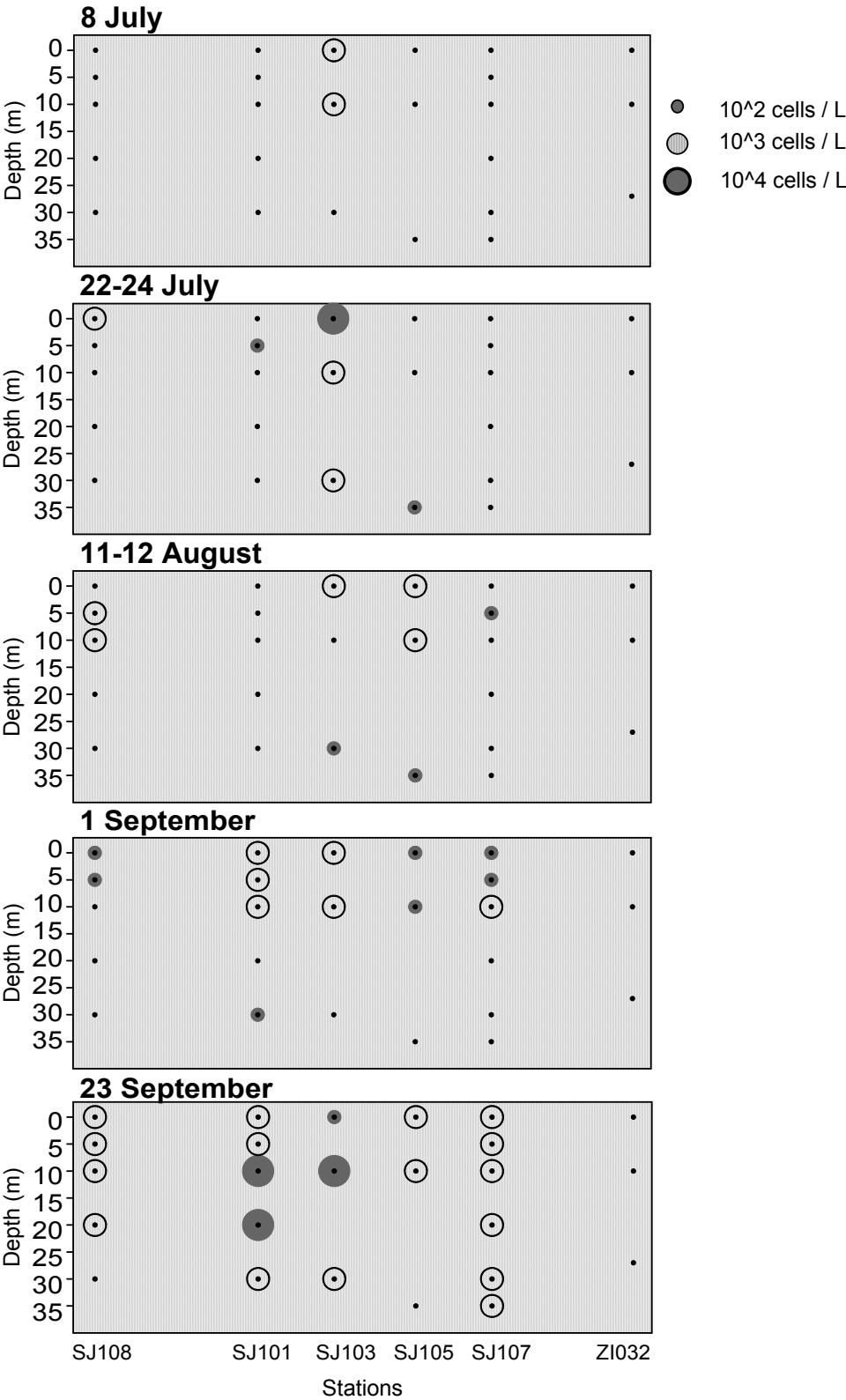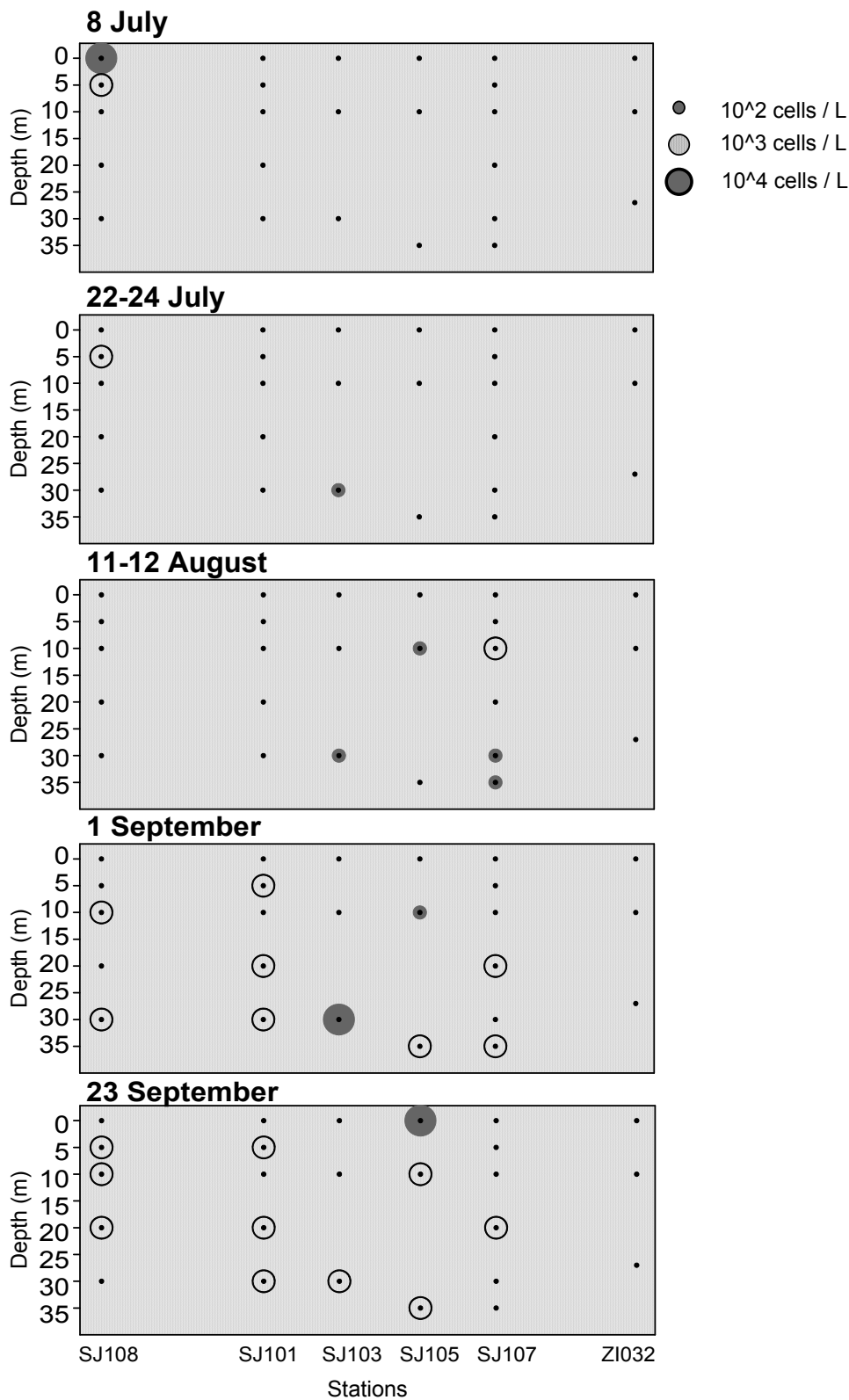
804

805 Fig. 6. Vertical distribution of *Cylindrotheca closterium* at the Po River delta − Rovinj profile on 8

806 July, 22–24 July, 11–12 August, 1 September and 23 September.

807

808

809

810

811

812

813

814

815

816

817

818

819

820

821

822

823

824

825

826

827   Fig. 7a. Total surface heat flux (Q) and flux due to evaporation (Q_e) along with wind speed (w) at Pula

828   station and daily Po river rates in July-September 1997. Fluxes are positive when the sea gains heat.

829   The grid lines coincide with sampling dates of the 8 July, the 22-24 July and the 11-13 August cruises.

830

831
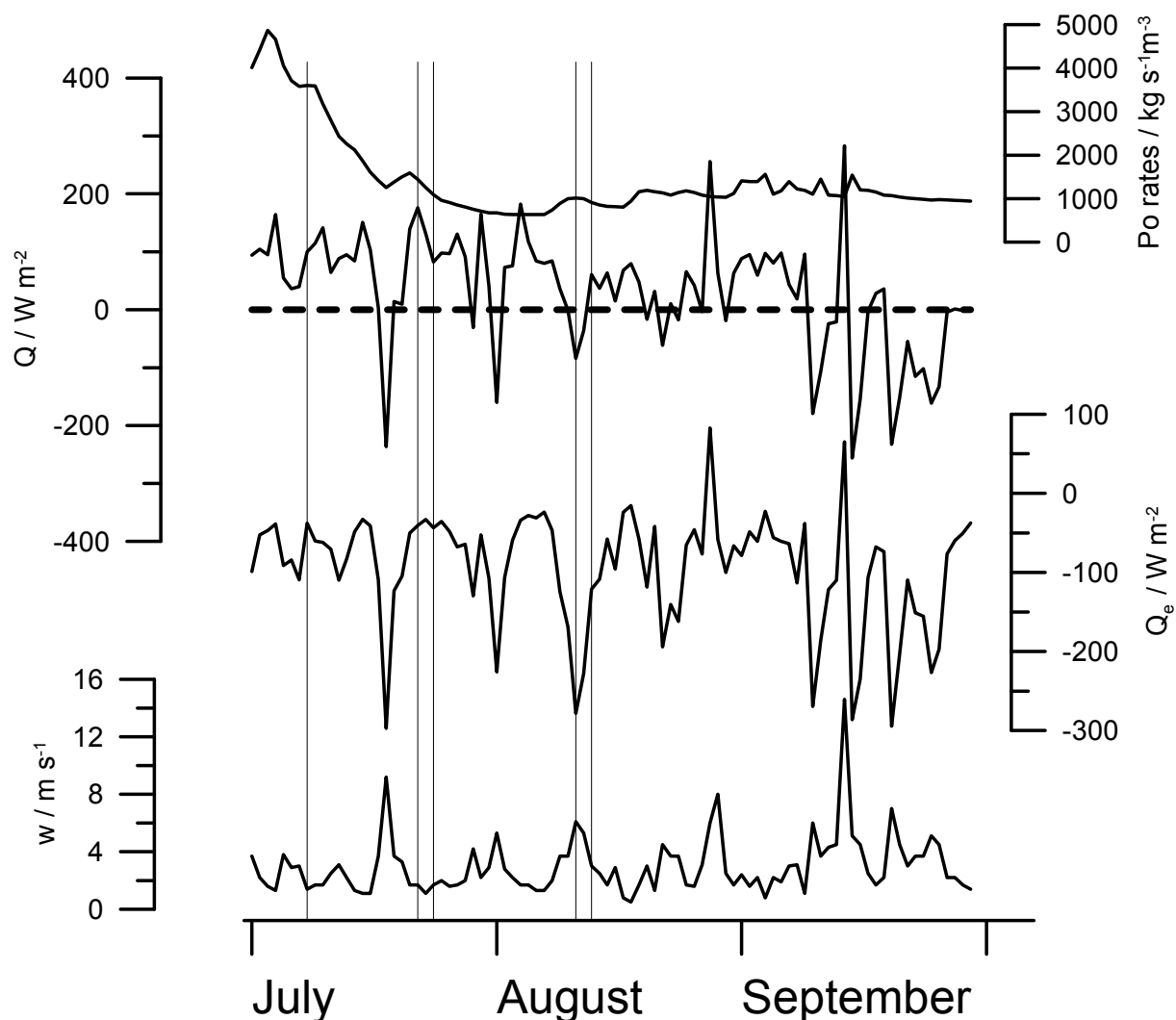
832   Fig. 7b. Sigma-t values at vertical section between SJ108 and RV001 on (a) 8 July, (b) 22-24 July

833   and (c) 11-13 August.

834
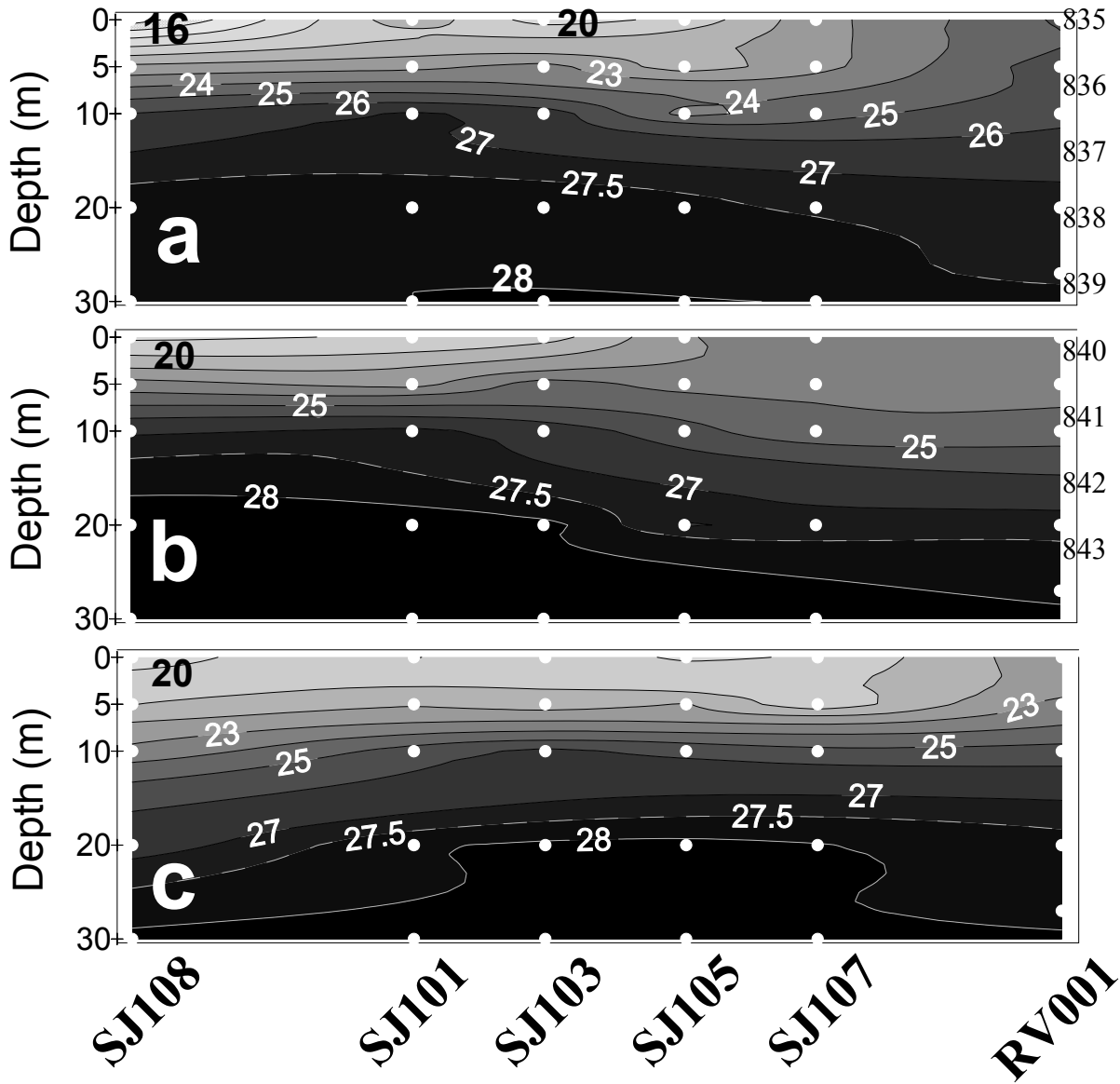
844   Fig. 8. Salinity (in blue) and dynamic depths of the 30-dbar surface (in grey) at 0 m, 10 m and 20 m on 22-24 July and 11-13 August.
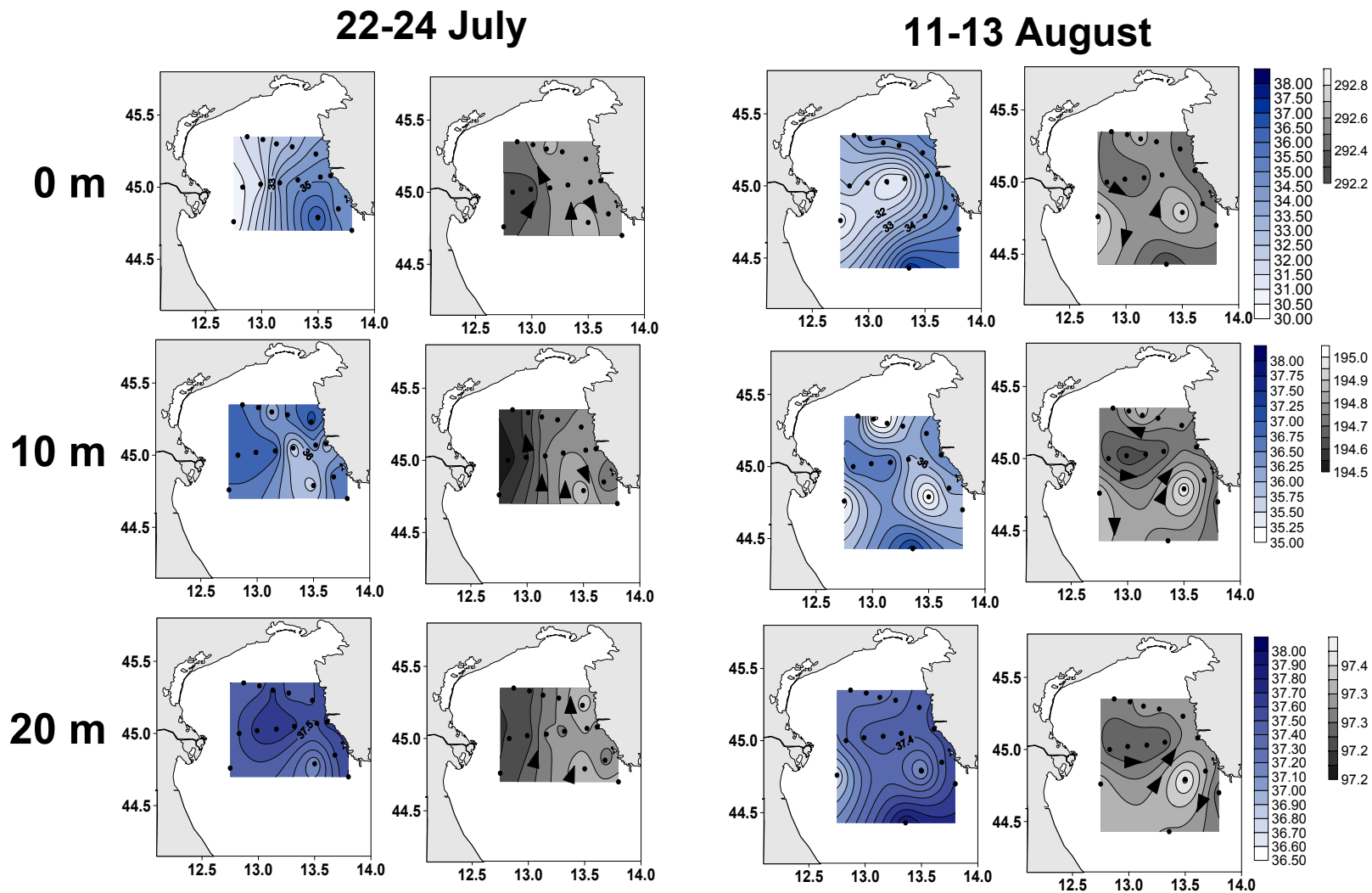
845

846

Kraus, Romina; Supić, Nastjenjka (2015) *Sea dynamics impacts on the macroaggregates: a case study of the 1997 mucilage event in the northern Adriatic*. Progress in Oceanography, 138 (A). pp. 249-267. (preprint version)

861

862 Table 6. Results of the PCA preformed on oceanographic parameters OP (Thermocline, Up temp –
863 temperature above thermocline, Up psal – salinity above thermocline, Up dene – density above
864 thermocline, Lo temp – temperature below thermocline, Lo psal – salinity below thermocline, Lo dene
865 – density below thermocline, Dene (Up-Lo) – difference between densities above and below
866 thermocline, Strat 30 – difference between densities in the 0 and 30 layers, Strat 10 – difference
867 between densities in the 0 and 10 layers, Dyn dpth 30 – dynamic depth of the 30 dbar surface, Dyn
868 dpth 20 – dynamic depth of the 20 dbar surface) for all stations with OP data sampled during cruises
869 on 8 July, 22-24 July and 11-13 August 1997 with parameter Origin (can be 1 or 0) indicating whether
870 the station is hypothetical origin of macroaggregate. Values in table represent contributions (loadings)
871 of each investigated parameter to first (PC1) and second (PC2) principal component. Results of higher
872 significancy are marked with bold or grey while n.s. means "not significant".

	8 July		22-24 July		11-13 August	
	PC1	PC2	PC1	PC2	PC1	PC2
Thermocline	-0,69	n.s.	-0,84	n.s.	n.s.	n.s.
Up temp	**0,94**	n.s.	0,76	n.s.	-0,61	n.s.
Up psal	**-0,99**	n.s.	**-0,98**	n.s.	**0,96**	n.s.
Up dene	**-0,99**	n.s.	**-0,97**	n.s.	**0,96**	n.s.
Lo temp	-0,83	n.s.	-0,56	n.s.	0,79	n.s.
Lo psal	-0,80	n.s.	-0,89	n.s.	0,82	n.s.
Lo dene	n.s.	-0,52	n.s.	0,89	n.s.	0,89
Dene (Up-Lo)	**1,00**	n.s.	**0,94**	n.s.	**-0,99**	n.s.
Strat 30	**0,97**	n.s.	**0,95**	n.s.	**-0,96**	n.s.
Strat 10	**0,91**	n.s.	**0,95**	n.s.	-0,78	n.s.
Dyn dpth 30	0,46	n.s.	-0,78	n.s.	n.s.	n.s.
Dyn dpth 20	0,58	n.s.	-0,60	n.s.	-0,59	n.s.
Origin	n.s.	0,67	0,59	n.s.	-0,63	n.s.

885 Suppl. 1. List of 128 phytoplankton seawater samples collected during July, August and September

886 1997. Phytoplankton seawater samples from July and August are clustered into 13 SPGs (in brackets).

887 For seawater samples in September SPGs were not determined.

888

8.7.	0	SJ108, SJ103 and SJ105 (2), SJ101 and SJ107 (9)
	5	SJ108 (12), SJ101 (8), SJ107 (9)
	10	SJ108 (8), SJ101 and SJ107 (9), SJ103 and SJ105 (12)
	20	SJ108 and SJ101 (2), SJ107 (12)
	bottom	SJ108 (1), SJ103 (2), SJ101, SJ105 and SJ107 (12)
22.7.	0	SJ101 and SJ103 (4), SJ108, SJ105 and SJ107 (13)
	5	SJ101 (4), SJ108 and SJ107 (12)
	10	SJ108, SJ101, SJ103, SJ105 and SJ107 (12)
	20	SJ108, SJ101 and SJ107 (12)
	bottom	SJ108, SJ101, SJ103, SJ105 and SJ107 (12)
23.7.	0	SJ001 and SJ007 (4), ZI012 (13)
	10	SJ001 and SJ007 (12), ZI012 (13)
	bottom	SJ001 (7) SJ007 (12), ZI012 (13)
24.7.	0	ZI032 (13)
	10	ZI032 (13)
	bottom	ZI032 (13)
11.8.	0	SJ108, SJ101, SJ103, SJ105 and SJ107 (4)
	5	SJ108, SJ101 and SJ107 (4)
	10	SJ108 and SJ107 (4), SJ105 (5), SJ101 and SJ103 (13)
	20	SJ107 (11), SJ101 (12), SJ108 (13)
	bottom	SJ107, 30m (3), SJ108 (4), SJ105 (10), SJ107, 35m (12), SJ101 and SJ103 (13)
12.8.	0	SJ007 (4), ZI012 (5)
	10	SJ007 (4), ZI012 (13)
	bottom	ZI012 (6), SJ007 (7)
1.9.	0	SJ108, SJ101, SJ103, SJ105, SJ107
	5	SJ108, SJ101, SJ107
	10	SJ108, SJ101, SJ103, SJ105, SJ107
	20	SJ108, SJ101, SJ107
	bottom	SJ108, SJ101, SJ103, SJ105, SJ107
23.9.	0	SJ108, SJ101, SJ103, SJ105, SJ107
	5	SJ108, SJ101, SJ107
	10	SJ108, SJ101, SJ103, SJ105, SJ107
	20	SJ108, SJ101, SJ107
	bottom	SJ108, SJ101, SJ103, SJ105, SJ107

889

890

891 Suppl. 2. Basic statistics (average, standard deviation, min and max) of the OP (Thermocline – thermocline depth, Up temp – temperature above

892 thermocline, Up psal – salinity above thermocline, Up dene – density above thermocline, Lo temp – temperature below thermocline, Lo psal –

893 salinity below thermocline, Lo dene – density below thermocline, Dene (Up-Lo) –above and below thermocline, Strat 30 – difference between

894 densities in the 0 and 30 layers, Strat 10 – difference between densities in the 0 and 10 layers, Dyn dpth 30 – dynamic depth of the 30 dbar surface,

895 Dyn dpth 20 – dynamic depth of the 20 dbar surface) for all stations with OP data sampled during cruises on 8 July, 22-24 July and 11-13 August

896 1997 calculated for: all stations (all available data), origin stations (stations where macroaggregates hypothetically formed), sampling stations

897 (stations where macroaggregates were sampled) and non-origin stations (stations where hypothetically no macroaggregates were formed).

898

Date		All stations	Origin stations	Sampling stations	Non-origin stations
8 July	Thermocline	11,25±4,11 (7,50-15,00)	7,50±0,00 (7,50-7,50)		13,10±3,80 (7,50-15,00)
	Up temp	23,02±0,62 (21,87-23,58)	23,23±0,29 (23,03-23,44)		22,92±0,76 (21,87-23,58)
	Up psal	32,80±2,51 (29,13-36,64)	32,30±0,82 (31,72-32,88)		33,06±3,17 (29,13-36,64)
	Up dene	22,26±2,06 (19,33-25,50)	21,82±0,54 (21,44-22,20)		22,49±2,60 (19,33-25,50)
	Lo temp	14,50±1,12 (13,46-16,65)	14,01±0,77 (13,46-14,55)		14,75±1,29 (13,93-16,65)
	Lo psal	36,93±0,28 (36,42-37,17)	36,89±0,11 (36,81-36,97)	no macroaggregates were sampled on 8 July	36,95±0,35 (36,42-37,17)
	Lo dene	27,56±0,24 (27,27-27,83)	27,64±0,08 (27,58-27,70)		27,52±0,29 (27,27-27,83)
	Dene (Up-Lo)	5,29±2,08 (1,77-7,94)	5,82±0,46 (5,50-6,14)		5,03±2,62 (1,77-7,94)
	Strat 30	6,95±3,17 (2,17-11,53)	7,45±1,63 (6,29-8,60)		6,70±3,95 (2,17-11,53)
	Strat 10	4,71±3,35 (0,62-9,61)	6,31±1,25 (5,42-7,19)		3,91±3,96 (0,62-9,61)
	Dyn dpth 30	292,44±0,16 (292,28-292,67)	292,32±0,03 (292,30-292,34)		292,50±0,06 (292,28-292,67)
	Dyn dpth 20	195,14±0,16 (194,93-195,38)	195,04±0,04 (195,02-195,07)		195,19±0,19 (194,93-195,38)
22-24 July	Thermocline	13,75±4,47 (7,50-25,00)	10,50±4,10 (7,50-15,00)	10,50±4,11 (7,50-15,00)	15,20±3,90 (7,50-25,00)
	Up temp	24,11±0,48 (23,47-25,33)	24,51±0,55 (23,96-25,33)	24,53±0,60 (23,63-25,33)	23,92±0,33 (23,47-24,50)
	Up psal	34,35±1,22 (32,05-35,52)	33,58±1,50 (32,05-35,44)	33,30±1,45 (32,05-35,04)	34,70±0,96 (32,50-35,52)
	Up dene	23,12±1,03 (21,02-24,10)	22,42±1,26 (21,02-23,99)	22,20±1,24 (21,02-23,78)	23,44±0,78 (21,61-24,10)
	Lo temp	15,53±1,50 (13,17-17,93)	15,52±1,31 (13,95-16,98)	15,00±1,22 (13,95-16,73)	15,54±1,64 (13,17-17,93)
	Lo psal	37,50±0,20 (37,18-37,80)	37,35±0,16 (37,18-37,59)	37,31±0,18 (37,18-37,63)	37,57±0,18 (37,19-37,80)
	Lo dene	27,75±0,31 (27,24-28,37)	27,65±0,26 (27,30-27,99)	27,73±0,26 (27,30-27,99)	27,80±0,33 (27,24-28,37)
	Dene (Up-Lo)	4,63±1,15 (3,29-6,69)	5,23±1,46 (3,51-6,69)	5,54±1,38 (4,02-6,69)	4,36±0,93 (3,29-6,27)
	Strat 30	6,12±1,52 (4,22-8,59)	7,15±1,68 (4,66-8,27)	7,27±1,87 (4,52-8,59)	5,74±1,35 (4,22-8,59)
	Strat 10	3,31±2,31 (0,17-7,17)	4,32±2,93 (0,63-7,17)	4,20±3,51 (0,17-7,17)	2,85±1,96 (0,17-7,08)
	Dyn dpth 30	292,42±0,10 (292,23-292,62)	292,34±0,10 (292,23-292,46)	292,35±0,10 (292,27-292,48)	292,45±0,09 (292,23-292,62)
	Dyn dpth 20	195,14±0,08 (194,99-195,27)	195,11±0,10 (194,99-195,25)	195,13±0,09 (195,03-195,25)	195,15±0,07 (195,03-195,27)
11-13 August	Thermocline	15,16±3,22 (7,50-25,00)	15,00±0,00 (15,00-15,00)	15,00±0,00 (15,00-15,00)	15,30±4,20 (7,50-25,00)
	Up temp	24,95±0,84 (22,90-26,32)	25,19±0,59 (24,52-26,19)	24,76±1,21 (22,90-26,19)	24,81±0,96 (22,90-26,32)
	Up psal	34,76±1,38 (32,39-37,38)	33,90±0,95 (32,71-34,97)	34,33±1,78 (32,71-37,10)	35,27±1,37 (32,39-37,38)
	Up dene	23,17±1,23 (20,97-25,54)	22,44±0,76 (21,25-23,18)	22,90±1,65 (21,25-25,54)	23,60±1,29 (20,97-25,54)
	Lo temp	15,47±1,23 (13,56-17,66)	14,34±0,87 (13,56-15,50)	14,62±1,09 (13,56-16,03)	16,15±0,87 (14,49-17,66)
	Lo psal	37,42±0,23 (37,02-37,91)	37,30±0,16 (37,02-37,46)	37,28±0,17 (37,02-37,46)	37,49±0,24 (37,16-37,91)
	Lo dene	27,72±0,23 (27,39-28,17)	27,89±0,30 (27,39-28,17)	27,89±0,32 (27,39-28,14)	27,62±0,10 (27,50-27,80)
	Dene (Up-Lo)	4,55±1,29 (2,03-6,55)	5,44±0,71 (4,53-6,30)	4,90±1,72 (2,03-6,30)	4,02±1,29 (2,03-6,55)
	Strat 30	5,96±1,66 (2,87-8,59)	7,26±1,35 (5,28-8,59)	7,48±1,13 (6,07-8,59)	5,09±1,24 (2,87-7,64)
	Strat 10	2,41±1,97 (0,12-5,77)	3,88±1,60 (1,38-5,76)	3,48±1,49 (1,29-5,14)	1,53±1,67 (0,12-5,77)
	Dyn dpth 30	292,53±0,11 (292,30-292,79)	292,54±0,06 (292,49-292,65)	292,54±0,07 (292,49-292,65)	292,53±0,14 (292,30-292,79)
	Dyn dpth 20	195,20±0,15 (194,89-195,49)	195,27±0,12 (195,19-195,49)	195,22±0,22 (194,89-195,49)	195,17±0,15 (194,89-195,40)

899 Suppl. 3a,b,c. Running cumulative total (Cumul.) of the sequential tests on variables and dbRDA

900 coordinate scores (dbRDAx; x - depending on number of identified variables in sequential tests) of the

901 DISTLM preformed with (1) seawater phytoplankton samples from the stations SJ001, SJ007, SJ101,

902 SJ103, SJ105, SJ107, SJ108, ZI012 and ZI032 sampled at 0 m, 10 m and bottom and (2) variables:

903 Thermocline, Up temp – temperature above thermocline, Up psal – salinity above thermocline, Up

904 dene – density above thermocline, Lo temp – temperature below thermocline, Lo psal – salinity below

905 thermocline, Lo dene – density below thermocline, Dene (Up-Lo) – difference between densities above

906 and below thermocline, Strat 10 – difference between densities in the 0 and 10 layers, Dyn dpth 20 –

907 dynamic depth of the 20 dbar surface with or without parameter Origin (can be 1 or 0) indicating

908 whether the station is hypothetical origin of macroaggregate on 8 July (Date 1), 22-24 July (Date 2)

909 and 11-13 August 1997 (Date 3). Unless specified, results were the same with or without parameter

910 Origin (origin included or origin excluded, respectively) from the analysis. Marked + in column Origin

911 denotes the location of the hypothetical origin of macroaggregate/s. Variable on grey points out those

912 that are found most important for analysed samples. dbRDA coordinate score on grey indicates the

913 highest value for each sample included in a DISTLM analysis for a specific depth and date.

914

915

916 Suppl. 3a.

Date 1								
	0 m			**10 m**			**Bottom**	
Variable	**Cumul.**		**Variable**	**Cumul.**		**Variable**	**Cumul.**	
Up psal	0,46		Lo psal	0,73		Strat 10	0,69	
Lo psal	0,88		Strat 10	0,88		Lo psal	0,93	
Lo temp	0,96		Up psal	0,97				

Origin	Sample	dbRDA1	dbRDA2	dbRDA3	dbRDA1	dbRDA2	dbRDA3	dbRDA1	dbRDA2
+	SJ101-1	-37,92	-1,82	5,41	11,49	9,77	1,69	-13,77	3,87
+	SJ103-1	25,19	-0,16	-4,12	-23,80	5,01	-5,99	36,93	-18,74
	SJ105-1	18,55	-16,95	1,58	-21,16	-12,01	1,24	no data	no data
	SJ107-1	-28,49	3,51	-6,74	-7,25	2,80	5,43	-50,19	-4,44
	SJ108-1	22,67	15,41	3,87	40,72	-5,57	-2,37	27,03	19,32

918   Suppl. 3b.

	Date 2			

0 m (origin excluded)		0 m (origin included)		10 m	Bottom

Variable	Cumul.	Variable	Cumul.	Variable	Cumul.	Variable	Cumul.
Strat 10	0,48	Strat 10	0,48	Lo dene	0,68	Lo dene	0,47
Dyn dpth 20	0,61	Origin	0,62			Up temp	0,76
Lo temp	0,77	Dyn dpth 20	0,75			Lo psal	0,85
Lo dene	0,86	Up temp	0,86				
Thermocline	0,92	Lo psal	0,91				
Lo psal	0,95						

Origin	Sample	dbRDA1	dbRDA2	dbRDA3	dbRDA4	dbRDA5	dbRDA6	dbRDA1	dbRDA2	dbRDA3	dbRDA4	dbRDA5	dbRDA1	dbRDA1	dbRDA2	dbRDA3
+	SJ001-2	30,02	2,30	2,74	-2,10	1,08	-0,37	20,90	-2,60	2,06	0,43	-1,01	0,28	-36,70	8,44	-2,33
	SJ007-2	15,11	3,23	-3,38	1,23	-1,09	-0,79	15,01	-2,51	-6,56	0,93	0,77	1,52	22,67	-5,37	0,10
+	SJ101-2	20,63	-0,69	-5,40	-0,10	0,16	0,10	31,28	3,78	1,09	0,06	-0,02	21,48	13,95	7,90	-1,62
+	SJ103-2	12,21	-7,16	2,19	-0,29	-0,20	0,89	10,21	4,82	2,24	-1,09	0,55	4,02	15,11	-1,71	0,13
	SJ105-2	-24,54	-9,95	0,91	1,62	0,78	-0,66	-23,31	8,95	-0,28	0,57	-0,52	-0,97	no data	no data	no data
	SJ107-2	-33,10	2,16	-5,90	-3,15	-0,09	0,12	-33,66	0,12	-0,98	0,16	0,19	7,76	22,73	2,00	4,55
	SJ108-2	-2,89	4,83	-3,36	3,01	0,45	0,64	-4,18	-1,65	-6,77	-1,11	-0,47	12,75	21,44	-2,48	-5,29
+	ZI012-2	-16,86	10,56	7,51	0,38	-0,01	0,02	-10,79	-13,24	3,60	-0,09	0,04	-30,91	-40,36	-8,79	-1,25
+	ZI032-2	-0,57	-5,26	4,70	-0,60	-1,07	0,05	-5,47	2,33	5,61	0,13	0,48	-15,94	-18,85	0,00	5,72

919

920   Suppl. 3c.

Date 3

0 m		10 m (origin excluded)		10 m (origin		Bottom	
Variable	Cumul.	Variable	Cumul.	Variable	Cumul.	Variable	Cumul.
Dene (Up-Lo)	0,50	Dyn dpth 20	0,34	Origin	0,42	Lo psal	0,44
Up psal	0,78	Lo psal	0,56			Dene (Up-Lo)	0,64
Lo temp	0,92	Lo temp	0,73			Up temp	0,84
Thermocline	0,95	Lo dene	0,85			Strat 10	0,94
Up dene	0,98						

Origin	Sample	dbRDA1	dbRDA2	dbRDA3	dbRDA4	dbRDA5	dbRDA1	dbRDA2	dbRDA3	dbRDA4	dbRDA1	dbRDA1	dbRDA2	dbRDA3	dbRDA4
+	SJ007-3	15,35	17,60	3,04	-0,94	0,28	-20,79	11,80	7,32	1,73	-10,23	30,09	-10,56	-19,03	10,45
+	SJ101-3	-6,49	6,19		2,29	-0,80	10,89	-13,84	11,42	2,91	-10,23	0,73	1,25	2,08	-7,97
	SJ103-3	-10,19	-1,96	-2,07	-1,88	-1,57	19,55	-0,14	3,08	-2,71	25,58	-8,70	-3,29	-10,02	-17,51
+	SJ105-3	-4,12	8,58	-2,54	0,43	0,55	-0,58	-7,48	-15,34	1,88	-10,23	no data	no data	no data	no data
+	SJ107-3	-10,99	-6,06	-2,52	-0,61	1,73	-27,16	-1,15	-2,13	3,20	-10,23	6,02	34,67	2,85	4,36
+	SJ108-3	-7,22	-9,55	8,11	0,37	-0,01	-10,17	-1,51	-0,61	-8,93	-10,23	-50,75	-7,89	1,07	9,93
	ZI012-3	23,65	-14,81	-2,44	0,34	-0,18	28,26	12,32	-3,73	1,92	25,58	22,62	-14,18	23,05	0,73

936 **References**

937 Aktan, Y., Dede, A., Ciftci, P.S., 2008. Mucilage event associated with diatoms and dinoflagellates in

938 Sea of Marmara, Turkey. Harmful Algae News - An IOC Newsletter on toxic algae and algal blooms,

939 http://ioc.unesco.org/hab/news.htm.

940 Alcoverro, T., Conte, E., Mazzella, L., 2000. Production of mucilage by the Adriatic epipelic diatom

941 *Cylindrotheca closterium* (Bacillariophyceae) under nutrient limitation. J Phycol 36, 1087-1095.

942 Alldredge, A.L., 1976. Discarded appendicularian houses as sources of food, surface habitats, and

943 particulate organic matter in planktonic environments. Limnol Oceanogr 21 (l), 14-23.

944 Alldredge, A.L., 1999. The potential role of particulate diatom exudates in forming nuisance

945 mucilaginous scums. Ann Ist Super Sanità 35, 397-400.

946 Alldredge, A.L., Crocker, K.M., 1995. Why do sinking mucilage aggregates accumulate in the water

947 column? Sci Total Environ 165, 15-22.

948 Alldredge, A.L., Silver, M.W., 1988. Characteristics, dynamics and significance of marine snow. Prog

949 Oceanogr 20, 41-82.

950   Blažina, M., Najdek, M., Fuks, D., Degobbis, D., 2005. Fatty acid profiling of microbial community
951   during aging of mucilaginous aggregates in the northern Adriatic. Sci Total Environ 336 (1-3), 91-103.

952   Blažina, M., Najdek, M., Fuks, D., Smodlaka; N., 2011. Microbial communities in northern Adriatic
953   mucilaginous aggregates: insight into the early phase of aggregate formation. Hydrobiologia 658 (1),
954   213-220.

955   Calvo, S., Barone, R., Naselli, F.L., 1995. Observations on mucus aggregates along Sicilian coasts
956   during 1991-1992. Sci Total Environ 165, 23-32.

957   Cataletto, B., Feoli, E., Fonda Umani, S., Monti, M., Pecchiar, I., 1996. Analyses of the relationship
958   between mucous aggregates and phytoplankton communities in the Gulf of Trieste (Northern Adriatic
959   Sea) by multivariate techniques. Mar Ecol 17, 291-308.

960   Cozzi, S., Ivančić, I., Catalano, G., Đakovac, T., Degobbis, D., 2004. Dynamics of the oceanographic
961   properties during mucilage appearance in the Northern Adriatic Sea: analysis of the 1997 event in
962   comparison to earlier events. J Mar Syst 50: 223-241.

963   Danovaro, R., Umani, S.F., Pusceddu, A., 2009. Climate change and the potential spreading of marine
964   mucilage and microbial pathogens in the mediterranean sea. PLoS ONE 4 (9), e7006.
965   doi:10.1371/journal.pone.0007006.

966   Decho, A.W., Herndl, G., 1995. Microbial activities and the transformation of organic matter within
967   mucilaginous material. Sci Total Environ 165, 33-42.

968   Degobbis, D., 1989. Increased eutrophication of the northern Adriatic sea. Second act. Mar Pollut Bull
969   20, 452-457.

970   Degobbis, D., Fonda-Umani, S., Franco, P., Malej, A., Precali, R., Smodlaka, N., 1995. Changes in the
971   northern Adriatic ecosystem and the hypertrophic appearance of gelatinous aggregates. Sci Total
972   Environ 165, 43-58.

973   Degobbis, D., Malej, A., Fonda-Umani, S., 1999. The mucilage phenomenon in the northern Adriatic.
974   A critical review of the present scientific hypotheses. Ann Ist Super Sanità 35, 373-381.

975 Degobbis, D., Precali, R., Ivančić, I., Smodlaka, N., Fuks, D., Kveder, S., 2000. Long-term changes in
976 the northern Adriatic ecosystem related to anthropogenic eutrophication. Int J Environ and Pollut 13,
977 495-533.

978 De Jonge, V.N., Van Beuselom, J.E.E., 1992. Contribution of resuspended microphytobenthos to total
979 phytoplankton in the EMS estuary and its possible role for grazers. Neth J Sea Res 30, 91-105.

980 De Jonge, V.N., Van Beusekom, J.E.E., 1995. Wind- and tide-induced resuspension of sediment and
981 microphytobenthos from tidal flats in the Ems estuary. Limnol Oceanogr 40 (4), 766-778.

982 De Lazzari, A., Berto, D., Cassin, D., Boldrin, A., Giani, M., 2008. Influence of winds and
983 oceanographic conditions on the mucilage aggregation in the Northern Adriatic Sea in 2003–2006. Mar
984 Ecol 29, 469–482.

985 Del Negro, P., Crevatin, E., Larato, C., Ferrari, C., Totti, C., Pompei, M., Giani, M., Berto, D., Fonda
986 Umani, S., 2005. Mucilage microcosms. Sci Tot Environ 353 (1-3), 258-269.

987 Flander Putrle, V., 2003. Phytoplankton biomarker pigments as an indicator of the trophic state of the
988 coastal sea. Doctoral dissertation Thesis. University of Ljubljana, Ljubljana, Slovenia, 158 pp.

989 Flander Putrle, V., Terzić, S., Malej, A., Ahel, M., 2000. Effects of mucilage event on the distribution
990 of summer phytoplankton as reflected by phytoplankton pigments. Period Biol 102 (2), 169-177.

991 Flander-Putrle, V., Malej, A., 2008. The evolution and phytoplankton composition of mucilaginous
992 aggregates in the northern Adriatic Sea. Harmful Algae 7 (6), 752-761.

993 Fogg, G.E., 1995. Some speculations on the nature of the pelagic mucilage community of the northern
994 Adriatic Sea. Sci Total Environ 165, 59-63.

995 Fonda Umani, S., Ghirardelli, E., Specchi, M., 1989. *Gli episodi di "mare sporco" nell'Adriatico dal
996 1729 ai giorni nostri* (eds.). Trieste, Regione Autonoma Friuli-Venezia Giulia. Direzione Regionale
997 dell'Ambiente p 178.

998 Fonda Umani, S., Milani, L., Borme, D., de Olazabal, A., Parlato, S., Precali, R., Kraus, R., Lučić, D.,
999 Njire, J., Totti, C., Romagnoli, T., Pompei, M., Cangini, M., 2005. Inter-annual variations of planktonic
1000 food webs in the northern Adriatic Sea and their role in driving organic carbon fluxes. Sci Tot Environ
1001 353 (1-3), 218-231.

1002   Franco, P., Michelato, A., 1992. Northern Adriatic Sea: oceanography of the basin proper and of the
1003   western coastal zone. Sci Total Environ Suppl., 35-62.

1004   Giani, M., Berto, D., Zangrando, V., Castelli, S., Sist, P., Urbani, R., 2005. Chemical characterization
1005   of different typologies of mucilaginous aggregates in the Northern Adriatic Sea. Sci Tot Environ 353
1006   (1-3), 232-246.

1007   Gotsis-Skretas, O., 1995. Mucilage appearance in Greek waters during 1982-1994. Sci Total Environ
1008   165, 229-230.

1009   Grossart, H.P., 1999. Interactions between marine bacteria and axenic diatoms (*Cylindrotheca
1010   fusiformis*, *Nitzschia laevis*, and *Thalassiosira weissflogii*) incubated under various conditions in the
1011   lab. Aquat Microb Ecol 19, 1-11.

1012   Herndl, G.J., 1992. Marine snow in the northern Adriatic Sea: possible causes and consequences for a
1013   shallow ecosystem. Mar Microb Food Webs 6, 149-172.

1014   Herndl, G.J., Peduzzi, P., 1988. Ecology of amorphous aggregations (marine snow) in the Northern
1015   Adriatic Sea: I. General considerations. P.S.Z.N.I: Mar Ecol 9, 79-90.

1016   Innamorati, M., 1995. Hyperproduction of mucilages by micro and macro algae in the Tyrrhenian Sea.
1017   Sci Total Environ 165, 65-81.

1018   Kaltenböck, E., Herndl, G.J., 1992. Ecology of amorphous aggregations (marine snow) in the Northern
1019   Adriatic Sea. IV. Dissolved nutrients and the autotrophic community associated with marine snow. Mar
1020   Ecol-Prog Ser 87, 147-159.

1021   Kovac, N., Bajt, O., Faganeli, J., Sket, B., Orel, B., 2002. Study of macroaggregate composition using
1022   FT-IR and H-1-NMR spectroscopy. Mar Chem 78, 205-215.

1023   Krajcar, V., 2003. The climatology of geostrophic currents in the northern Adriatic. Geofizika, 20,
1024   105-114.

1025   Kraus, R., Ivančić, I., Đakovac, T., Smodlaka, N., 2004. Northern Adriatic mesocosm experiment
1026   Rovinj 2003: Changes in the microphytoplankton community. Period Biol 106 (1), 31-37.

1027   Kraus, R., Supić., 2011. Impact of circulation on high phytoplankton blooms and fish catch in the
1028   northern Adriatic (1990-2004). Estuar Coast Shelf S 91(2), 198-210.

1029   Lancelot, C., 1995. The mucilage phenomenon in the continental coastal waters of the North Sea. Sci
1030   Tot Environ 165, 83-102.

1031   Lyons, D.M., Supić, N., Smodlaka, N., 2007. Geostrophic circulation patterns in the northeastern
1032   Adriatic Sea and the effects of air-sea coupling: May–September 2003. J Geophys Res, 112, C03S08.

1033   MacKenzie, L., Sims, I., Beuzenberg, V., Gillespie, P., 2002. Mass accumulation of mucilage caused
1034   by dinoflagellate polysaccharide exudates in Tasman Bay, New Zealand. Harmful Algae 1, 69-83.

1035   Mauri, E., Poulain, M.P., 2001. Surafce chlorophyll distribution and currents in
1036   the Adriatic in fall 1997 and winter 1998. J Mar Syst 29, 51-67.

1037   Monti, M., Welker, C., Fonda Umani, S., 1994. Particulate organic carbon analyses in three marine
1038   diatoms under controlled conditions. Giornale Botanico ltaliano 128, 1074-1077.

1039   Monti, M., Welker, C., Dellavalle, G., Casaretto, L., Fonda Umani, S., 1995. Mucous aggregates under
1040   natural and laboratory conditions: a review. Sci Total Environ 165, 145-154.

1041   Najdek, M., 1996. Fatty acid composition in amorphous aggregates in the northern Adriatic Sea. Mar
1042   Ecol-Prog Ser 139, 219-226.

1043   Najdek, M., Degobbis, D., Mioković, D., Ivančić, I., 2002. Fatty acid and phytoplankton composition
1044   of different types of mucilaginous aggregates in the northern Adriatic Sea. J Plankton Res 24 (5), 429-
1045   441.

1046   Najdek, M., Blažina, M., Đakovac, T., Kraus, R., 2005. The role of the diatom *Cylindrotheca*
1047   *closterium* in a mucilage event in the northern Adriatic Sea: coupling with high salinity water
1048   intrusions. J Plankton Res 27 (9), 851-862.

1049   Pistocchi, R., Trigari, G., Serrazanetti, G.P., Taddei, P., Monti, G., Palamidesi, S., Guerrini,
1050   F., Bottura, G., Serratore, P., Fabbri, M., Pirini, M., Ventrella, V., Pagliarani, A., Boni, L., Borgatti,
1051   A.R., 2005. Chemical and biochemical parameters of cultured diatoms and bacteria from the Adriatic
1052   Sea as possible biomarkers of mucilage production. Sci Total Environ 353 (1-3), 287-299.

1053   Precali, R., Giani, M., Marini, M., Grilli, F., Ferrari, C.R., Pečar, O., Paschini, E., 2005. Mucilaginous
1054   aggregates in the northern Adriatic in the period 1999–2002: Typology and distribution. Sci Total
1055   Environ 353 (1-3), 10-23.

1056   Revelante, N., Gilmartin, M., 1976. Temporal succession of phytoplankton in the northern Adriatic.
1057   Neth J Sea Res 10, 377–396.

1058   Revelante, N., Williams, W.T., Gilmartin, M., 1984. A numerical assessment of the temporal and
1059   spatial distribution of phytoplankton assemblages in the northern Adriatic sea. J Exp Mar Biol Ecol 77
1060   (1-2), 137-150.

1061   Revelante, N., Gilmartin, M., 1991. The phytoplankton composition and population enrichment in
1062   gelatinous "macroaggregates" in the northern Adriatic during the summer of 1989. J Exp Mar Biol
1063   Ecol 146, 217-233.

1064   Rinaldi, A., Vollenweider, R.A., Montanari, G., Ferrari, C.R., Ghetti, A., 1995. Mucilages in Italian
1065   seas - the Adriatic and Tyrrhenian seas, 1988-1991. Sci Total Environ 165, 165-183.

1066   Russo, A., Maccaferri, S., Đakovac, T., Precali, R., Degobbis, D., Deserti, M., Paschini, E., Lyons, D.,
1067   2005. Meteorological and oceanographic conditions in the northern Adriatic Sea during the period June
1068   1999 - July 2002: influence on the mucilage phenomenon. Sci Total Environ 353 (1-3), 24-38.

1069   Stachowitsch, M., Fanuko, N., Richter, M., 1990. Mucus aggregates in the northern Adriatic Sea: an
1070   overview of types and occurrences. PSZNI Mar Ecol 11, 327-350.

1071   Supić, N., Orlić, M., 1999. Seasonal and interannual variability of the northern Adriatic surface fluxes.
1072   J Mar Syst 20, 205-229.

1073   Supić, N., Orlić, M., Degobbis, D., 2000. Istrian Coastal Countercurrent and its Year-to-Year
1074   Variability. Estuar Coast Shelf S 51 (3), 385-397.

1075   Supić N., Orlić, M., Degobbis, D., Đakovac, T., Krajcar, V., Precali, R., 2001-2002. Occurrence of the
1076   Istrian Coastal Countercurrent (ICCC) in 2000, a year with a mucilage event. Geofizika 18-19, 45-57.

1077   Supić N., Orlić, M., Degobbis, D., 2003. Istrian Coastal Countercurrent in the year 1997. Il Nuovo
1078   Cimento 26 (2), 117-131.

1079   Supić, N., Vilibić, I., 2006. Dense water characteristics in the northern Adriatic in the 1967-2000
1080   interval with respect to surface fluxes and Po river discharge rates. Estuar Coast Shelf S 66, 580-593.

1081   Supić, N., Kraus, R., Kuzmić, M., Paschini, E., Precali, R., Russo, A., Vilibić, I., 2012. Predictability
1082   of northern Adriatic winter conditions, J Mar Syst 90, 42-57.

1083   Thornton, D.C.O., 2002. Diatom aggregation in the sea: mechanisms and ecological implications. Eur
1084   J Phycol 37: 149-161.

1085   Totti, C., Cangini, M., Ferrari, C., Kraus, R., Pompei, M., Pugnetti, A., Romagnoli, T., Vannucci, S.,
1086   Socal, G., 2005. Phytoplankton size-distribution and community structure in relation to mucilage
1087   occurrence in the northern Adriatic Sea. Sci Total Environ 353 (1-3), 204-217.

1088   Tüfekçi, V., Balkis, N., Polat Beken, Ç., Ediger D., Mantikçi, M., 2010. Phytoplankton composition
1089   and environmental conditions of a mucilage event in the Sea of Marmara. Turk J Biol, 34, 199-210,
1090   doi:10.3906/biy-0812-1.

1091   Urbani, R., Magaletti, E., Sist, P., Cicero, A.M., 2005. Extracellular carbohydrates released by the
1092   marine diatoms *Cylindrotheca closterium*, *Thalassiosira pseudonana* and *Skeletonema costatum*:
1093   Effect of P-depletion and growth status. Sci Total Environ 353 (1-3), 300-306.

1094   Utermöhl, H., 1958. Zur Verfollkommnung der quantitativen Phytoplankton-Methodik. Mitt Int Verein
1095   theor angew Limnol 17, 47-71.

1096   Vilibić I., Beg Paklar, G., Žagar, N., Mihanović, H., Supić, N., Žagar, M., Domijan, N., Pasarić, M.,
1097   2008. Summer breakout of trapped bottom dense water from the northern Adriatic, J Geophys Res
1098   113, 1-19.

1099   Welker, C., Monti, M., 1994. Polysaccharidic flocculation from the marine diatom *Cylindrotheca*
1100   *closterium* (Ehr.) Reimann & Lewin under nutrient starvation. Giornale Botanico ltaliano 128, 1078-
1101   1081.